



**HAL**  
open science

# Chemical engineering around the 5,12-dihydroindolo[3,2a]carbazole scaffold: Fine tuning of the optical properties of visible light photoinitiators of polymerization

Fatima Hammoud, Akram Hijazi, Malika Ibrahim-Ouali, Jacques Lalevée,  
Frédéric Dumur

## ► To cite this version:

Fatima Hammoud, Akram Hijazi, Malika Ibrahim-Ouali, Jacques Lalevée, Frédéric Dumur. Chemical engineering around the 5,12-dihydroindolo[3,2a]carbazole scaffold: Fine tuning of the optical properties of visible light photoinitiators of polymerization. *European Polymer Journal*, 2022, pp.111218. 10.1016/j.eurpolymj.2022.111218 . hal-03661753

**HAL Id: hal-03661753**

**<https://hal.science/hal-03661753>**

Submitted on 7 May 2022

**HAL** is a multi-disciplinary open access archive for the deposit and dissemination of scientific research documents, whether they are published or not. The documents may come from teaching and research institutions in France or abroad, or from public or private research centers.

L'archive ouverte pluridisciplinaire **HAL**, est destinée au dépôt et à la diffusion de documents scientifiques de niveau recherche, publiés ou non, émanant des établissements d'enseignement et de recherche français ou étrangers, des laboratoires publics ou privés.

# Chemical engineering around the 5,12-dihydroindolo[3,2-*a*]carbazole scaffold : Fine tuning of the optical properties of visible light photoinitiators of polymerization

Fatima Hammoud<sup>1,2,3</sup>, Akram Hijazi<sup>3</sup>, Malika Ibrahim-Ouali<sup>4</sup>, Jacques Lalevée<sup>1,2\*</sup> and Frédéric Dumur<sup>5\*</sup>

<sup>1</sup> Université de Haute-Alsace, CNRS, IS2M UMR 7361, F-68100 Mulhouse, France

<sup>2</sup> Université de Strasbourg, France

<sup>3</sup> EDST, Université Libanaise, Campus Hariri, Hadath, Beyrouth, Liban

<sup>4</sup> Aix Marseille Univ, CNRS, Centrale Marseille, iSm2, F-13397 Marseille, France

<sup>5</sup> Aix Marseille Univ, CNRS, ICR UMR 7273, F-13397 Marseille, France

\* Correspondence: [Jacques.lalevee@uha.fr](mailto:Jacques.lalevee@uha.fr), [frederic.dumur@univ-amu.fr](mailto:frederic.dumur@univ-amu.fr)

## Abstract

5,12-Dihydroindolo[3,2-*a*]carbazole is a promising scaffold for the design of visible light photoinitiators of polymerization due to the simultaneous presence of two carbazole moieties that can be differently functionalized. Notably, redshift of the absorption spectra can be easily obtained by nitration of one of the two carbazoles, the second carbazole group being functionalized with various groups. Dinitration of 5,12-dihydroindolo[3,2-*a*]carbazole is another efficient approach for designing dyes with strong absorptions extending over the visible range. In this work, a series of 36 compounds never reported in the literature and differing by the substitution pattern have been designed and synthesized. Notably, the possibility to design push-pull dyes by Knoevenagel and Claisen Schmidt reactions, to introduce electroactive groups such as thiophene by Suzuki cross-coupling reactions or to design water soluble chromophore has been explored. To evidence the interest of these structures, photopolymerization experiments have been carried out at 405 nm and the polymerization of acrylates has been examined in thick and thin films. To support the polymerization efficiency, mechanisms involved in the free radical polymerization of acrylates have been established by the combination of various techniques including UV-visible absorption and fluorescence spectroscopy, cyclic voltammetry and photolysis experiments.

## Keywords

Carbazole, photopolymerization, dyes, asymmetric substitution

## 1. Introduction

In recent years, visible light photopolymerization has been the focus of intense research efforts due to the wide range of applications in which this polymerization technique is involved.[1–6] Among the most popular applications, 3D printing, dentistry or microelectronics have boosted the development of new photoinitiators.[7–16] With aim at designing visible light photoinitiators, two competitive approaches can be developed.[17] The first one is based on the chemical modification of historical UV photoinitiators aiming at red-shifting their absorption towards the visible range.[18–20] However, considering that these chromophores were UV-centered, shift of their absorptions towards the visible range can only be obtained at the cost of difficult syntheses and most of the dyes only absorb not far from the near-UV/visible range.[21–29] Face to these considerations, a second approach consists in developing new molecules totally disconnected from these historical structures.[30–48] Considering that visible light photoinitiators of polymerization should exhibit a strong absorption over the visible range, long-living excited state lifetimes but also appropriate electrochemical properties in order to efficiently interact with the different additives introduced into the photocurable resins, structures commonly used in Organic Electronics are candidates of choice for photoinitiation.[49] In this field, carbazole is a popular structure in Organic Electronics and interest for this structure is supported by the easiness of chemical modification, its good photochemical and thermal stability, good electron-donating ability, high triplet energy level[50,51] and wide bandgap.[52] Thus, carbazole can be used for the design of small-molecules and polymeric hosts for triplet emitters in Organic Light Emitting Diodes,[51,53–56], molecular glasses for organic and hybrid solar cells,[57–60] solid-state emitters for two-photon imaging,[61] chromophores for Non-Linear optical applications,[62–65] semiconductors for Organic Field Effect Transistors (OFETs),[66–68] Aside from Organic Electronics, carbazole can also be used for the design of compounds exhibiting biological activities (antihistaminic, antitumor, antiepileptic, anti-inflammatory, antimicrobial, antidiarrheal, analgesic and neuroprotective properties).[69] Carbazole has also been extensively used in photopolymerization,[70] acting as an electron donor in push-pull dyes, [71–76], a conjugated spacer for triphenylamine and pyrene-based structures,[75,77] as an elemental building block for the design of polycyclic structures such as helicenes,[78] or as chromophore for Type I photoinitiators.[79]

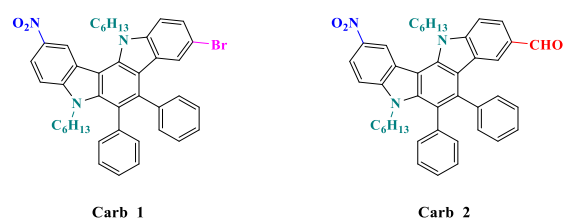
In 2019, an interesting structure combining within a unique molecule two carbazole moieties has been proposed, namely 5,12-dihydroindolo[3,2-*a*]carbazole.[80] In this pioneering

work, the symmetrical and regioselective *bis*(acetylation) and *bis*(formylation) at the C2,9-positions of the 5,12-dihydroindolo[3,2-*a*]carbazole core has been examined. However, absorptions of the resulting dyes were strongly UV-centered. Only in 2022, first attempts to asymmetrically substitute this structure have been reported.[81] Notably, the possibility to selectively nitrate one of the two carbazoles enabled first to redshift the absorption of the resulting dyes towards the visible range and second to introduce various groups onto the second carbazole such as formyl, acetyl, halogens that can advantageously be used for further chemical transformations. Asymmetrization of the substitution pattern is notably based on the difference of reactivity between the C2 and C9-positions, the C2-position being more reactive than the C9-position. Capitalizing on these preliminary results, a series of 30 dyes **Carb\_1-Carb\_36** based on the 5,12-dihydroindolo[3,2-*a*]carbazole scaffold have been designed and synthesized. Notably, innovative structures based on Suzuki cross-coupling reactions, Claisen-Schmidt and Knoevenagel reactions have been proposed. In fact, only **Carb\_1** and **Carb\_2** have been published in our previous work.[81] For all the other dyes i.e. **Carb\_3-Carb\_36**, none of these structures i.e. 33 compounds have previously been reported in the literature. To evidence the interest of these structures, the different dyes were used as Type II photoinitiators of polymerization upon photoactivation at 405 nm with a LED. The free radical polymerization of acrylates has been examined. Chemical mechanisms have been fully detailed by combining UV-visible absorption and fluorescence spectroscopy, photolysis experiments and cyclic voltammetry.

## 2. Synthesis of the different dyes

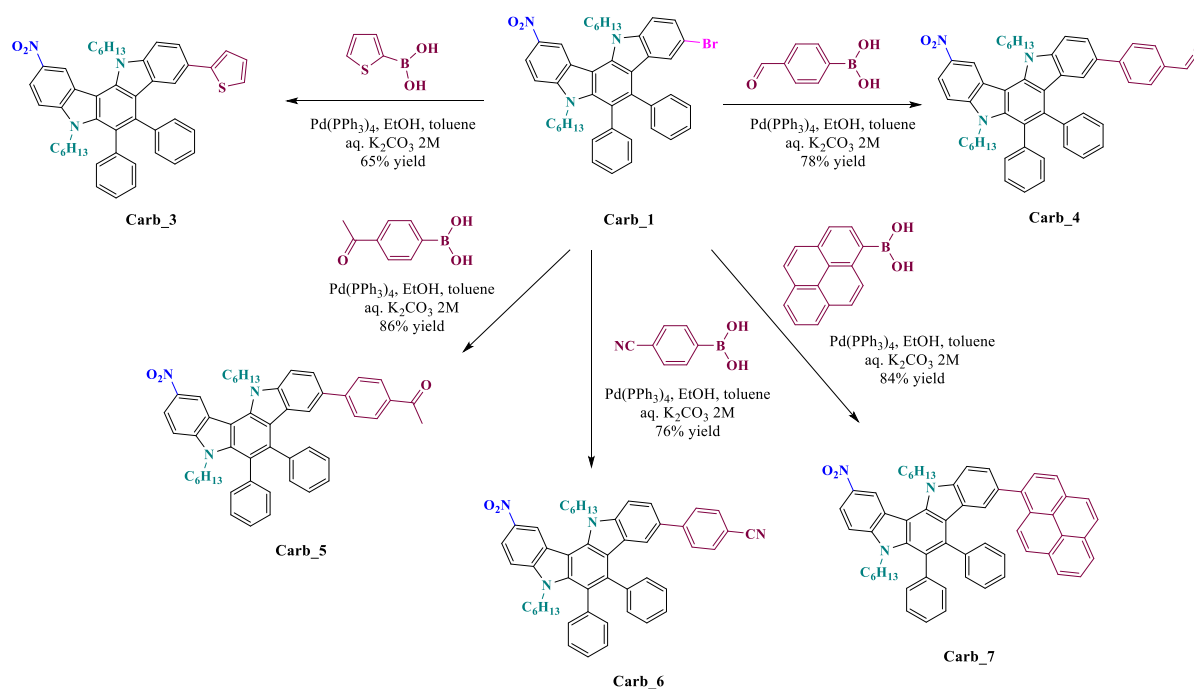
### 2.1. Synthesis of Carb\_1-Carb\_7 by Suzuki cross-coupling reactions

In this work, two structures, namely 9-bromo-5,12-dihexyl-2-nitro-6,7-diphenyl-5,12-dihydroindolo[3,2-*a*]carbazole **Carb\_1** and 5,12-dihexyl-2-nitro-6,7-diphenyl-5,12-dihydroindolo[3,2-*a*]carbazole-9-carbaldehyde **Carb\_2** previously reported in the literature [81] have been used as reagents for the design of new structures (See Scheme 1).



**Scheme 1.** Chemical structures of **Carb\_1** and **Carb\_2** used for the design of various dyes.

Due to the presence of bromine onto **Carb\_1**, Suzuki cross-coupling reactions could be carried out and **Carb\_3-Carb\_7** could be obtained with reaction yields ranging from 65 to 86% yields. Notably, electron-donating groups such as thiophene or pyrene, but also electron-withdrawing groups such as 4-formylphenyl, 4-acetylphenyl and 4-cyanophenyl substituents could be introduced as peripheral groups (See Scheme 2).



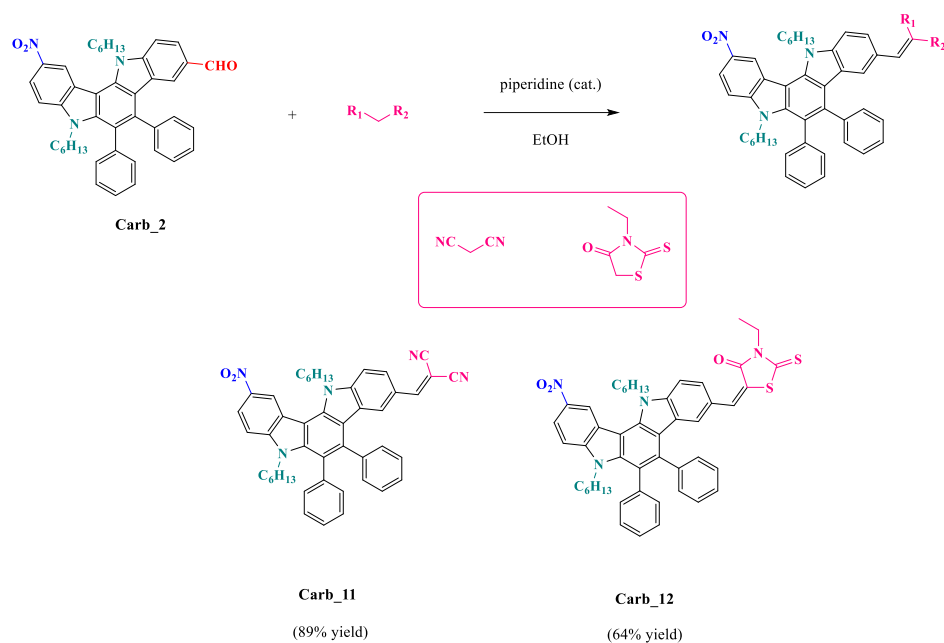
**Scheme 2.** Synthetic route to **Carb\_3-Carb\_7**.

## 2.2. Synthesis of push-pull dyes by Claisen-Schmidt and Knoevenagel reactions

By connecting an electron donor to an electron acceptor by mean of a  $\pi$ -conjugated spacer, the resulting molecules that are named push-pull dyes are characterized an intense and broad absorption band extending over the visible range, namely, the intramolecular charge transfer band.[82] In the context of visible light photopolymerization which requires dyes to absorb in the visible range, Claisen-Schmidt and Knoevenagel reactions are reactions of choice for the design of push-pull dyes.[42,83–87] Additionally, these reactions can be carried out in green conditions, an alcohol being used as the solvent and a few drops of amine are sufficient to catalyze the two reactions. To end, push-pull dyes can be easily recovered in pure form by precipitation in alcohols, facilitating the purification process.

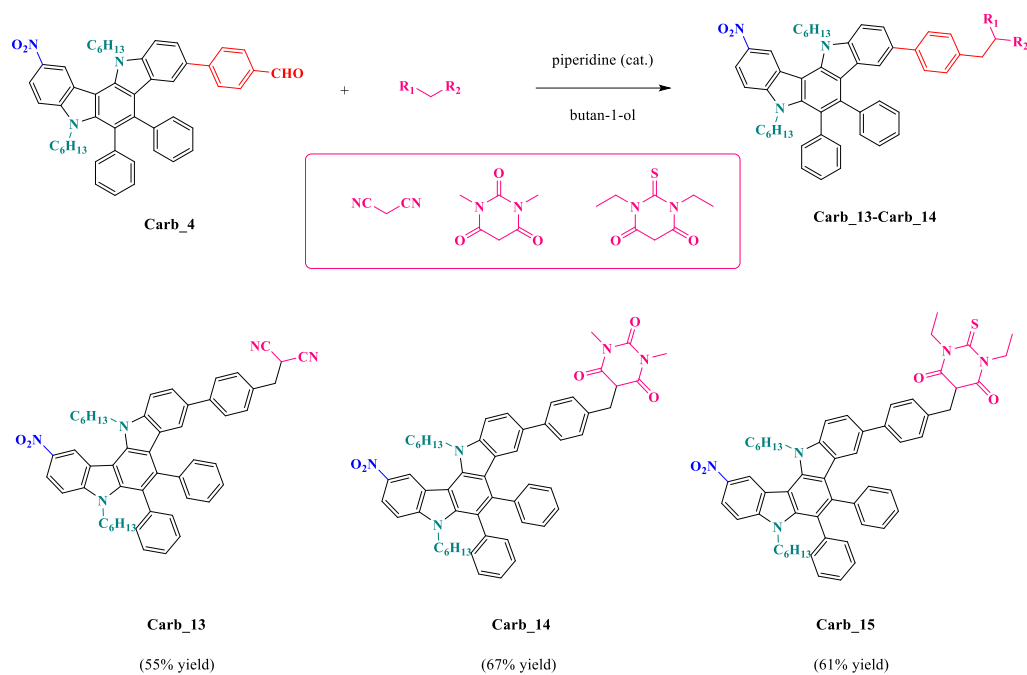
Thus, two dyes **Carb\_8** and **Carb\_9** were respectively prepared starting from **Carb\_2** and **Carb\_4** in 78 and 84% yields by a Claisen-Schmidt condensation of methyl picolinium iodide in butanol in the presence of a catalytic amount of piperidine (See Scheme 3). Noticeably,





**Scheme 4.** Synthetic routes to **Carb\_11-Carb\_12**.

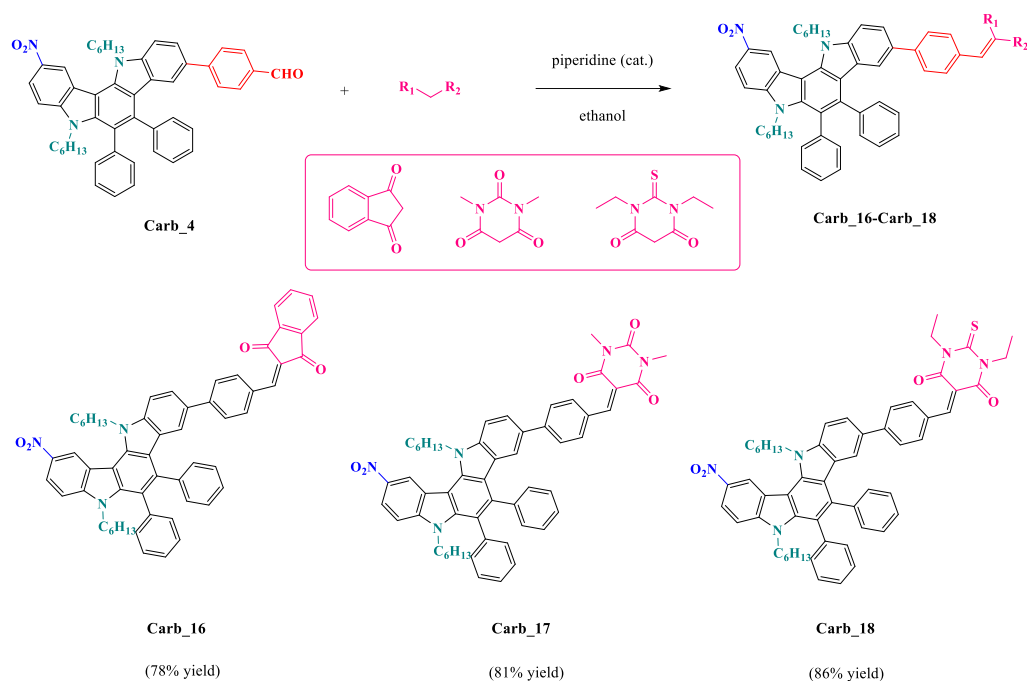
While performing the Knoevenagel reaction in butan-1-ol with **Carb\_4** as the aldehyde, an unexpected reaction occurred, furnishing **Carb\_13-Carb\_15** as the unique reaction products. The unexpected reduction reaction detected in butan-1-ol for **Carb\_13-Carb\_15** was assigned to the contamination of **Carb\_4** by traces of Pd(0) (Pd(0) is a side product of the Suzuki cross-coupling reaction), favouring the hydrogenation reaction subsequent to the Knoevenagel reaction.[88] Indeed, avoidance of trace catalysts residues is a major issue of organocatalyzed reactions.[89–93] The different dyes could be obtained with reaction yields ranging from 55% for **Carb\_13** to 67% for **Carb\_14** (See Scheme 5). Noticeably, all attempts to condense **Carb\_4** to indane-1,3-dione failed, the unique reaction product being the dimerization product of indane-1,3-dione, namely bindone.[66,67]



**Scheme 5.** Synthetic routes to **Carb\_13-Carb\_15**.

By performing the Knoevenagel reaction in ethanol exhibiting a lower boiling point, the targeted dyes **Carb\_16-Carb\_18** could be obtained with reaction yields ranging from 78 to 86% yields (See Scheme 6). Surprisingly, using ethanol as the solvent, no condensation reaction of **Carb\_4** was detected with malononitrile. Conversely, due to its lower boiling point, condensation of indane-1,3-dione with **Carb\_4** could be obtained, providing **Carb\_16** in 78% yield. Overall, it can be concluded that the undesired hydrogenation reaction observed during the synthesis of **Carb\_13-Carb\_15** results from the higher boiling point of butan-1-ol compared to ethanol used for **Carb\_16-Carb\_18**, around 40°C, favouring the hydrogenation reaction when butan-1-ol is used as the solvent.

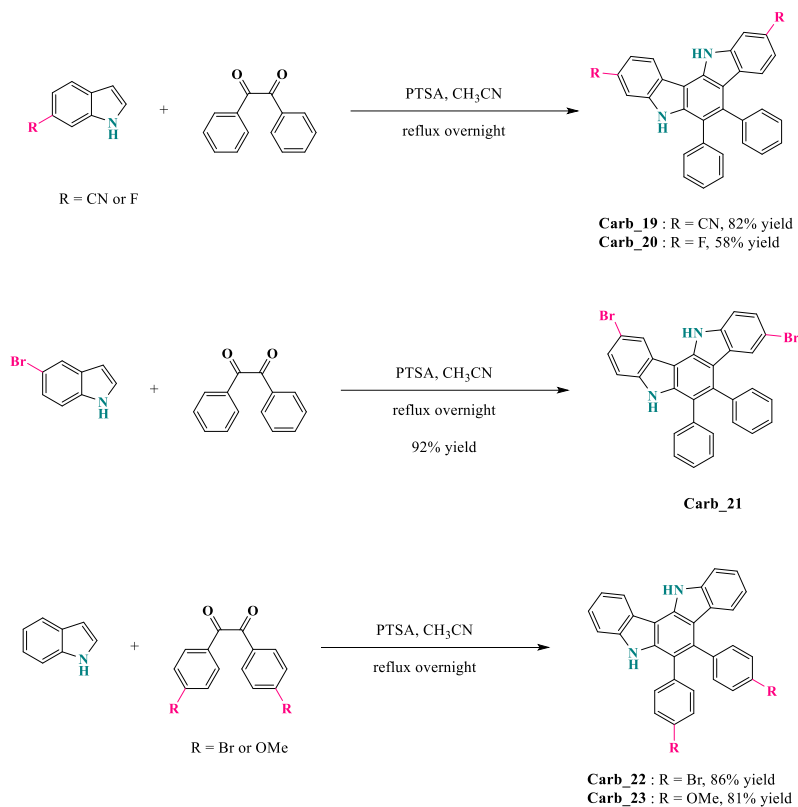




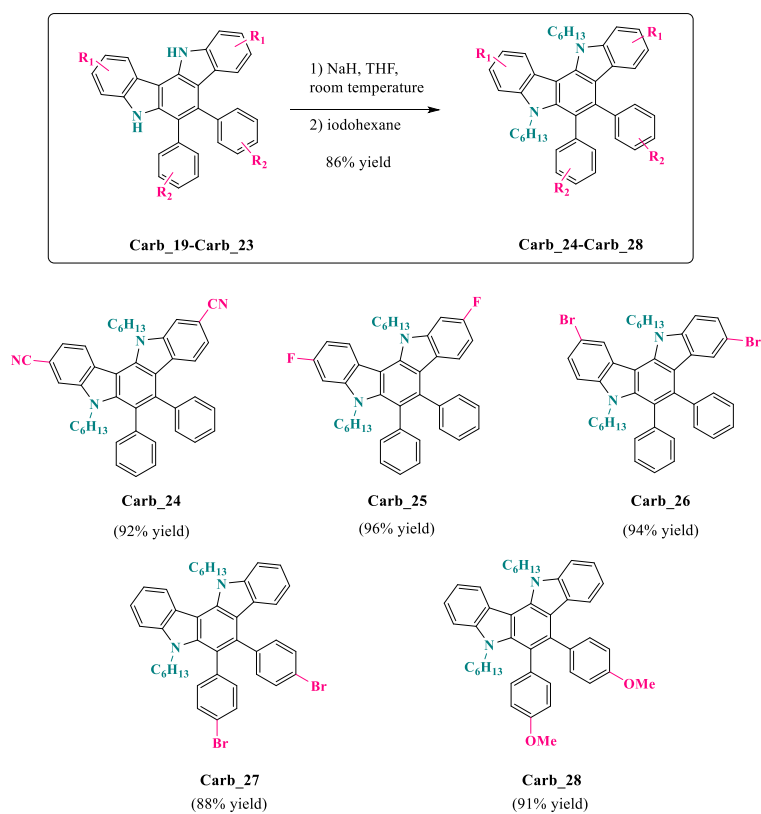
**Scheme 6.** Synthetic routes to **Carb\_16-Carb\_18**.

### 2.3. Syntheses of new 5,12-dihydroindolo[3,2-*a*]carbazole derivatives

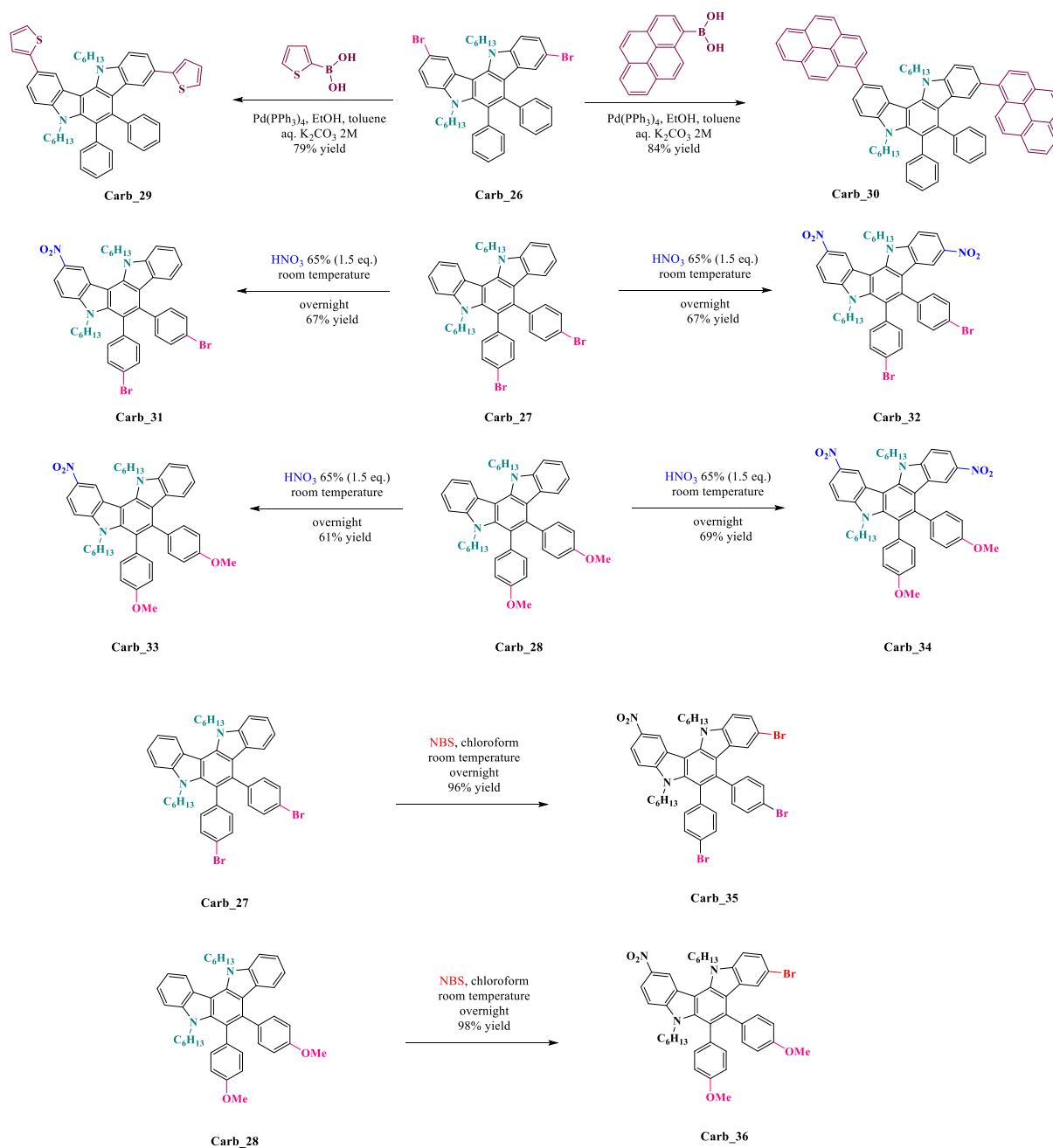
5,12-Dihydroindolo[3,2-*a*]carbazole is typically obtained by cycloaddition of two equivalents of indole with one equivalent of diphenylethanedione (benzil) in the presence of a catalytic amount of *para*-toluenesulfonic acid or RuO<sub>2</sub> nanoparticles (PTSA).[96–99] In this context, substituted indoles and benzils were examined as potential reagents for the design of unreported 5,12-dihydroindolo[3,2-*a*]carbazole derivatives. Notably, **Carb\_19-Carb\_23** could be obtained with reaction yields ranging from 58% for **Carb\_20** to 92% for **Carb\_21** (See Scheme 7). To improve the solubility of **Carb\_19-Carb\_23**, the different dyes were alkylated with iodohexane using sodium hydride as the base. All dyes **Carb\_25-Carb\_28** could be obtained in high yields (See Scheme 8). Due to the presence of two bromine atoms on **Carb\_26**, this compound was thus used for Suzuki cross-coupling reactions with 2-thienylboronic acid and 2-pyrenylboronic acid so that **Carb\_29** and **Carb\_30** could be obtained in 79 and 84% yields. Nitration of **Carb\_27** and **Carb\_28** was also examined and by controlling the number of equivalents of HNO<sub>3</sub> 65%, mono or *bis*-nitrated compounds **Carb\_31-Carb\_34** could be obtained in moderate yields. Notably, lower reaction yields were obtained during *bis*-nitration due to the formation of numerous side-products (See Scheme 9). Finally, considering that the heavy atom effect is important in photochemistry, **Carb\_31** and **Carb\_33** were brominated with NBS, providing **Carb\_35** and **Carb\_36** in almost quantitative yields.



**Scheme 7. Synthetic routes to Carb\_19-Carb\_23.**



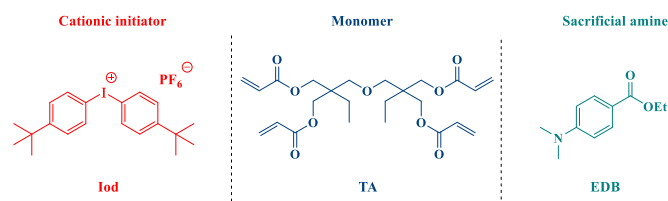
**Scheme 8. Synthetic routes to Carb\_24-Carb\_28.**



**Scheme 9.** Synthetic routes to Carb\_92-Carb\_36.

## 2.4. Other Chemicals compounds

*Bis*-(4-*tert*-butylphenyl)iodonium hexafluorophosphate (Iod; SpeedCure 938) was obtained from Lambson Ltd (UK). Ethyl 4-dimethylaminobenzoate (EDB; SpeedCure EDB) was obtained from Lambson. The monomer di(trimethylolpropane)tetraacrylate (TA)) was obtained from Allnex. Chemical structures of monomers and additives are shown in the Scheme 10.



**Scheme 10.** Chemical structures of monomers and additives used in this study.

## 2.5. Irradiation Source

The following light emitting diodes (LEDs) were used as irradiation sources: (i)  $\lambda_{em} = 405$  nm (denoted LED@405 nm) with an incident light intensity at the sample surface,  $I_0 = 110$  mW cm<sup>-2</sup> and (ii)  $\lambda_{em} = 375$  nm (denoted as LED@375 nm),  $I_0 = 40$  mW cm<sup>-2</sup>.

## 2.6. UV-visible absorption and photolysis experiments

UV-visible absorption properties of the different compounds ( $\sim 10^{-5}$  M) as well as the steady state photolysis experiments were studied using a JASCO V730 UV-visible spectrometer, in chloroform.

## 2.7. Photopolymerization kinetics (RT-FTIR)

Experimental conditions used for each photosensitive formulation are indicated in the caption of the figures. All polymerization tests were performed at room temperature and the irradiation was started at  $t = 10$  s. The weight content of the photoinitiating system is calculated from the monomer content. The photoinitiator concentrations in each photosensitive formulation have been chosen to ensure good light absorption at 405 nm. Conversion of the acrylate functions of TA was continuously followed by real time FTIR spectroscopy (JASCO FTIR 4100). For the thin samples ( $\sim 25$   $\mu$ m of thickness), free radical polymerizations of TA were performed in laminate (the formulation is sandwiched between two polypropylene films to reduce the O<sub>2</sub> inhibition). The decrease of C=C double bond band was continuously monitored from 1581 to 1662 cm<sup>-1</sup>. For the thicker samples ( $\sim 1.4$  mm of thickness), the formulations were deposited on a polypropylene film inside a 1.4 mm mold under air. Evolution of the C=C band and the epoxide group band were continuously followed from 6117 to 6221 cm<sup>-1</sup>.

## 2.8. Steady state fluorescence

Fluorescence spectra were acquired in a quartz cell at room temperature using a JASCO FP-750 spectrofluorometer. The same spectrometer was used for the fluorescence quenching experiments of the different dyes ( $\sim 10^{-5}$  M) in chloroform.

## 2.9. Redox potentials

Oxidation potentials ( $E_{ox}$ ) were measured in acetonitrile by cyclic voltammetry using tetrabutylammonium hexafluorophosphate (0.1 M) as the supporting electrolyte (potential vs. Saturated Calomel Electrode – SCE). The free energy change  $\Delta G_{et}$  for an electron transfer reaction was calculated from eqn (1), [100] where  $E_{ox}$ ,  $E_{red}$ ,  $E^*$ , and  $C$  are the oxidation potential of the electron donor (the carbazole derivatives), the reduction potential of the electron acceptor (the iodonium salt), the excited state energy and the coulombic term for the initially formed ion pair, respectively. Here,  $C$  is neglected for polar solvents.

$$\Delta G_{et} = E_{ox} - E_{red} - E^* + C \quad (\text{Eqn. 1})$$

## 2.10. Direct Laser Write

For direct laser write experiments, a laser diode emitting at 405 nm (spot size around 50  $\mu\text{m}$ ) was used for the spatially controlled irradiation. The photosensitive resin was polymerized under air and the generated 3D patterns were analyzed using a numerical optical microscope (DSX-HRSU from Olympus Corporation).

## 2.11. Near-UV Conveyor

Light-sensitive resins were deposited on the glass fibers used for reinforcement. Curing of the deposited resins was realized using an LED conveyor @ 395 nm ( $4 \text{ W/cm}^2$ ). The distance from the belt to the LED was set at 15 mm, and the belt speed was set at 2 m/min (3 s of irradiation per pass).

# 3. Results and discussion

## 3.1. UV-visible absorption properties of the different dyes

UV-visible absorption spectra of all dyes were recorded in chloroform as the solvent and the results are presented in the Figures 3-9. Different groups of molecules could be identified, depending on their absorption spectra. In the first group comprising **Carb\_1-Carb\_7**, all dyes comprise a nitro group in their scaffold enabling their absorptions to be centered in the visible range. For these dyes, an absorption maximum centered around 420 nm could be determined. The highest molar extinction coefficient was found for **Carb\_7** bearing a pyrene group as the substituent (See Figure 1 (A) and Table 1). Conversely, once an electron accepting group is connected to **Carb\_2**, a significant redshift of the absorption maxima could be found (See Figure 1 (B)). Thus, by improving the electron-withdrawing ability from **Carb\_11** to **Carb\_10**, position of the intramolecular charge transfer band shifted from 454 nm

for **Carb\_11** to 549 nm for **Carb\_10**. Interestingly, while comparing the absorption of **Carb\_8** and **Carb\_9** differing by the spacer between the carbazole structure and the pyridinium group, a blueshift of the absorption maxima was detected, the absorption peak shifting from 494 nm for **Carb\_8** to 447 nm for **Carb\_9**. This blueshift was assigned to the isolation of the electron donating carbazole in **Carb\_9** due to the consecutive presence of two phenyl groups that adversely affects the electronic delocalization.

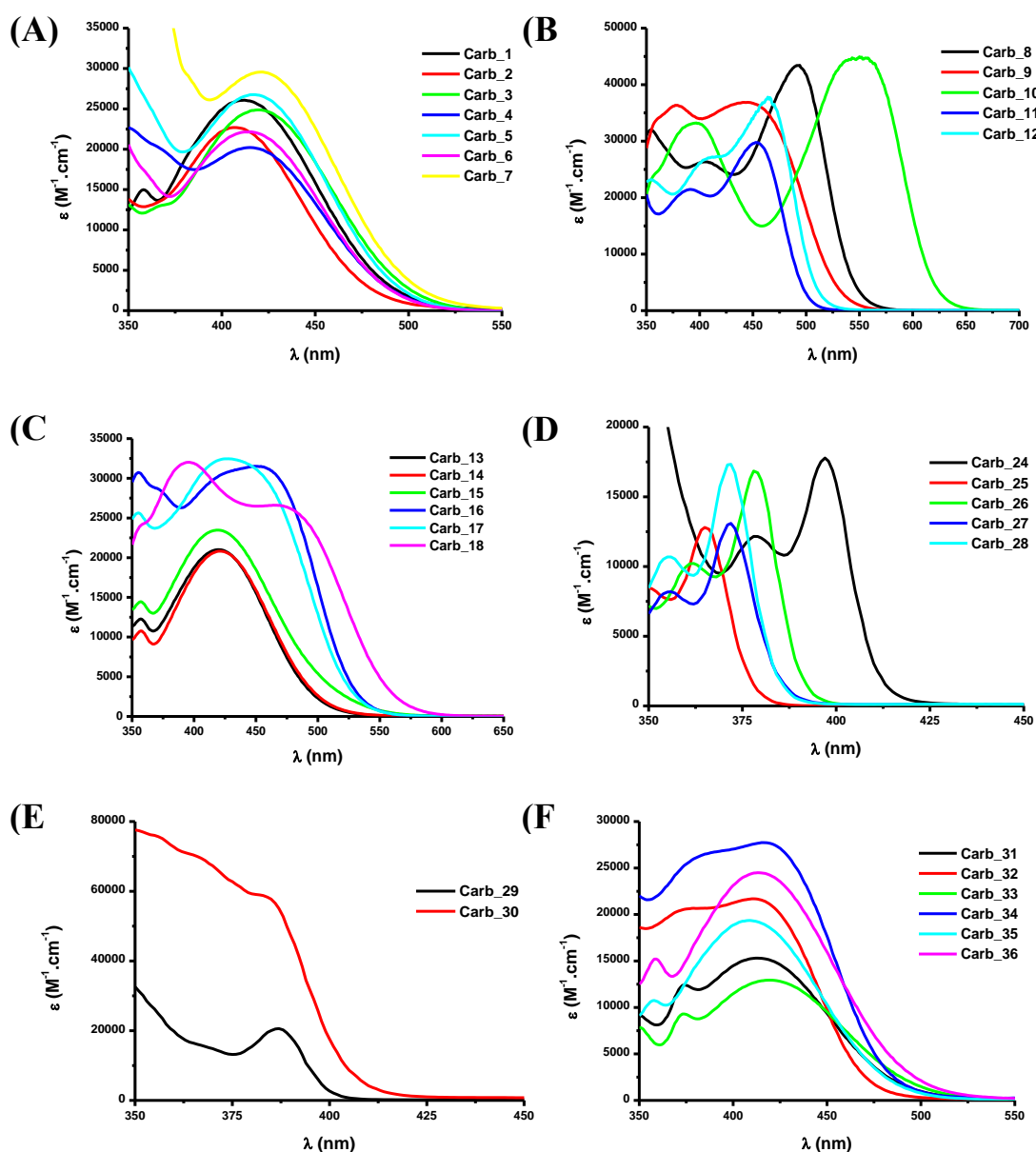


**Figure 1.** UV-visible absorption spectra of **Carb\_1- Carb\_30** in chloroform.

While comparing the absorption of **Carb\_13-Carb\_15** to that of **Carb\_17** and **Carb\_18**, replacement of the single bond in **Carb\_13-Carb\_15** by a double bond significantly

modified the absorption spectra compared to that of **Carb\_17** and **Carb\_18**. Due to the lack of conjugation with the electron accepting groups in **Carb\_13-Carb\_15**, similar absorption maxima peaking at 420 nm could be found for the three dyes. In the case of **Carb\_16-Carb\_18**, the lack of conjugation of the electron donating carbazole with the rest of the molecule was confirmed. Indeed, by improving the electron-withdrawing ability, almost no modification of the absorption maxima was found (See Figure 1 (C)).

By varying the substitution pattern of **Carb\_24-Carb\_28**, interesting trends could be determined. Thus, introduction of cyano groups onto **Carb\_24** enabled to produce a dye absorbing until 425 nm. Conversely, for **Carb\_25-Carb\_28**, almost no absorption was detected in the visible range, making these dyes poor candidates for photoinitiation in the visible range (See Figure 1 (D)). A similar deduction can be evidenced for **Carb\_29** and **Carb\_30** in which no electron-withdrawing groups have been introduced (See Figure 1 (E)).

Finally, introduction of one or two nitro groups onto **Carb\_31-Carb\_36** enabled to redshift the absorption spectra of these dyes compared to that of their parent structures **Carb\_26-Carb\_28** (See Figure 1 (F)). Interestingly, introduction of one or two nitro groups did not significantly modify the position of the absorption maxima, as shown in the **Table 1**.

**Table 1.** Optical characteristics of different dyes in chloroform as the solvent.

<b>PI</b>	<b>Carb_1</b>	<b>Carb_2</b>	<b>Carb_3</b>	<b>Carb_4</b>	<b>Carb_5</b>	<b>Carb_6</b>	<b>Carb_7</b>
$\lambda$ (nm)	410	407	420	416	417	416	421
$\epsilon$ (M <sup>-1</sup> .cm <sup>-1</sup> )	26100	22700	24600	20200	26750	22300	29600
<b>PI</b>	<b>Carb_8</b>	<b>Carb_9</b>	<b>Carb_10</b>	<b>Carb_11</b>	<b>Carb_12</b>	<b>Carb_13</b>	<b>Carb_14</b>
$\lambda$ (nm)	495	441	550	452	465	419	419
$\epsilon$ (M <sup>-1</sup> .cm <sup>-1</sup> )	43550	36700	45000	30000	37700	21000	21000
<b>PI</b>	<b>Carb_15</b>	<b>Carb_16</b>	<b>Carb_17</b>	<b>Carb_18</b>	<b>Carb_24</b>	<b>Carb_25</b>	<b>Carb_26</b>
$\lambda$ (nm)	418	453	428	469	397	365	379
$\epsilon$ (M <sup>-1</sup> .cm <sup>-1</sup> )	23500	31500	32500	26426	17550	12700	16800
<b>PI</b>	<b>Carb_27</b>	<b>Carb_28</b>	<b>Carb_29</b>	<b>Carb_30</b>	<b>Carb_31</b>	<b>Carb_32</b>	<b>Carb_33</b>
$\lambda$ (nm)	371	370	387	381	414	410	418
$\epsilon$ (M <sup>-1</sup> .cm <sup>-1</sup> )	12900	17200	20350	58700	15200	21700	12850
<b>PI</b>	<b>Carb_34</b>	<b>Carb_35</b>	<b>Carb_36</b>				
$\lambda$ (nm)	416	409	413				
$\epsilon$ (M <sup>-1</sup> .cm <sup>-1</sup> )	27700	19350	24500				

### 3.2. Free radical polymerization (FRP) of acrylates

Different combinations based on 5,12-dihydroindolo[3,2-*a*]carbazole derivatives (Carb/Iod, or Carb/EDB (0.1/1% w/w) and Carb/Iod/EDB (0.1%/1%/1% w/w/w)) have been tested for the FRP of TA in thin films (25  $\mu\text{m}$ , in laminate) and thick samples (1.4 mm, under air). High final acrylate function conversions (FCs) are shown for the different dyes while using the different photoinitiating systems (PISs) (Figures 2 and Table 2). It should be noted that the different dyes, Iod, or EDB examined separately were unable to initiate the FRP of TA under the same conditions, clearly showing that the presence of the dyes was required for an efficient process. For the Iod/EDB system (without Carb), a polymerization occurs in agreement with a Charge Transfer Complex (CTC) behavior. However, the polymerization rate is much slower and an inhibition time is found (Figure S1 in Supporting Information). Therefore, the presence of Carb clearly leads to better polymerization processes.

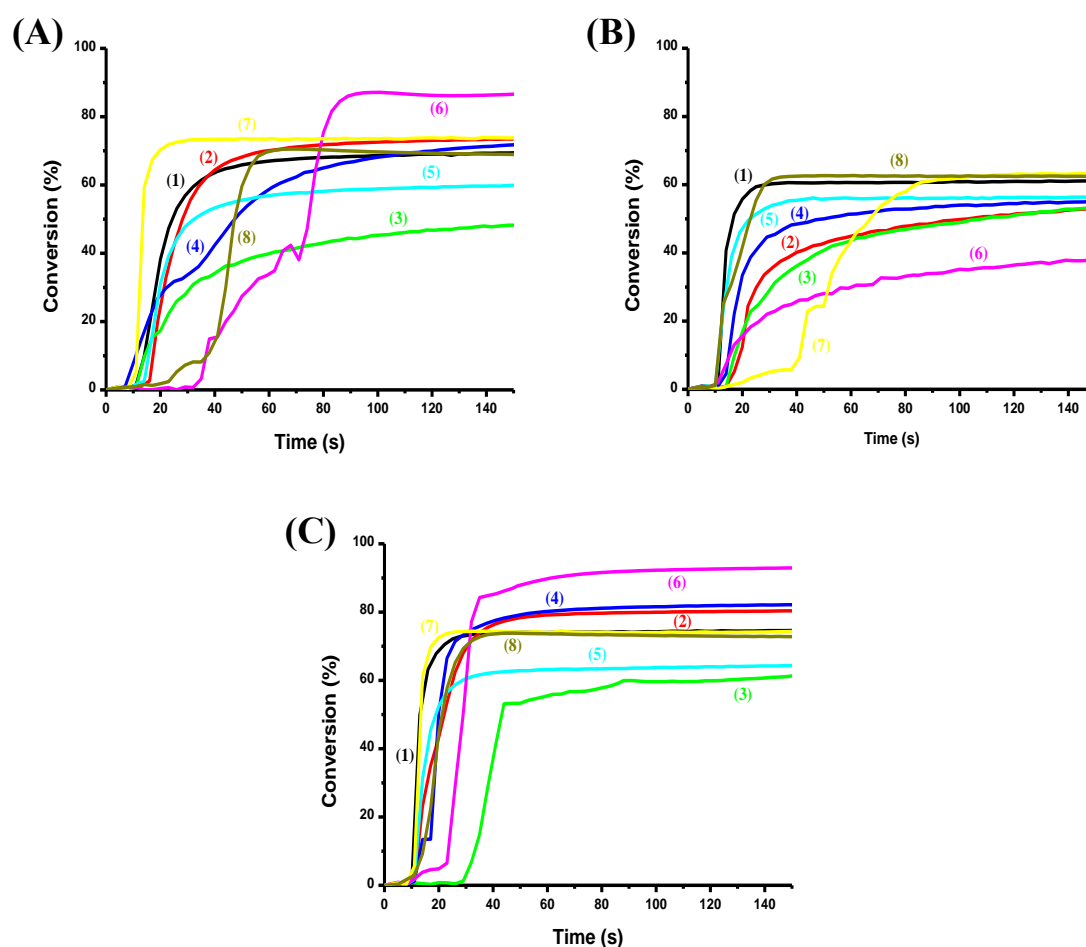


**Figure 2.** Photopolymerization profiles of TA (acrylate function conversion vs. irradiation time) in laminate (thickness = 25  $\mu\text{m}$ ) upon exposure to LED light  $\lambda = 405$  nm in the presence of two- and three-component photoinitiating systems based on carbazole compounds: (A) PI/Iod (0.1/1% w/w): (1)



Carb\_6/Iod, (2) Carb\_8/Iod, (3) Carb\_10/Iod, (4) Carb\_11/Iod, (5) Carb\_15/Iod, (6) Carb\_27/Iod, (7) Carb\_29/Iod, and (8) Carb\_36 (B) PI/EDB (0.1/1% w/w): (1) Carb\_6/EDB, (2) Carb\_8/EDB, (3) Carb\_10/EDB, (4) Carb\_11/EDB, (5) Carb\_15/EDB, (6) Carb\_27/EDB, (7) Carb\_29/EDB, and (8) Carb\_36/EDB (C) PI/Iod/EDB (0.1/1%/1% w/w/w): (1) Carb\_6/Iod/EDB, (2) Carb\_8/Iod/EDB, (3) Carb\_10/Iod/EDB, (4) Carb\_11/Iod/EDB, (5) Carb\_15/Iod/EDB, (6) Carb\_27/Iod/EDB, (7) Carb\_29/Iod/EDB, and (8) Carb\_36/Iod/EDB. The irradiation starts for t=10s.

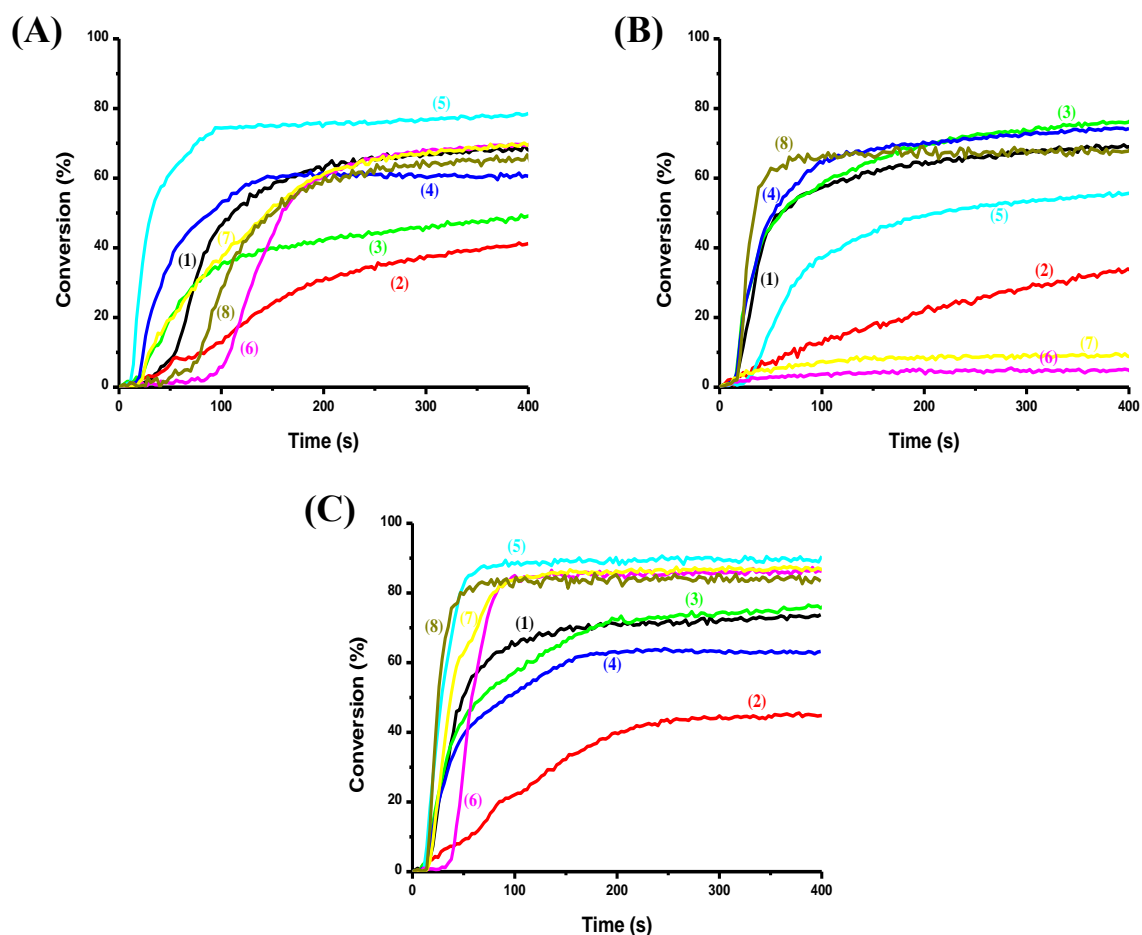
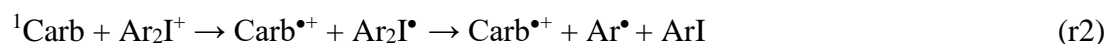
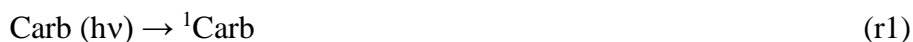


**Figure 3.** Photopolymerization profiles of TA (acrylate function conversion vs. irradiation time) under air (thickness = 1.4 mm) upon exposure to LED light  $\lambda = 405$  nm in the presence of two- and three-component photoinitiating systems based on carbazole compounds: (A) PI/Iod (0.1/1% w/w): (1) Carb\_5/Iod, (2) Carb\_8/Iod, (3) Carb\_13/Iod, (4) Carb\_15/Iod, (5) Carb\_24/Iod, (6) Carb\_27/Iod, (7) Carb\_30/Iod, and (8) Carb\_35 (B) PI/EDB (0.1/1% w/w): (1) Carb\_5/EDB, (2) Carb\_8/EDB, (3) Carb\_13/EDB, (4) Carb\_15/EDB, (5) Carb\_24/EDB, (6) Carb\_27/EDB, (7) Carb\_30/EDB, and (8) Carb\_35/EDB (C) PI/Iod/EDB (0.1/1%/1% w/w/w): (1) Carb\_5/Iod/EDB, (2) Carb\_8/Iod/EDB, (3) Carb\_13/Iod/EDB, (4) Carb\_15/Iod/EDB, (5) Carb\_24/Iod/EDB, (6) Carb\_27/Iod/EDB, (7) Carb\_30/Iod/EDB, and (8) Carb\_35/Iod/EDB. The irradiation starts for t=10s.

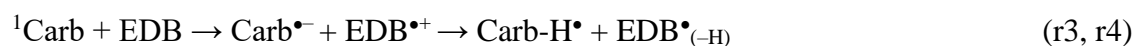
When the iodonium salt was combined with the different dyes, good photopolymerization profiles could be obtained (see Figure 2 (A), Figure 3 (A) and Table 2). In fact, the Carb/Iod interaction corresponds to an electron transfer reaction finally leading to

an aryl radical Ar• (r1) and (r2). Ar• is considered as the initiating species for the free radical polymerization:



FRP of TA in thin films (laminates) in the presence of the different Carb/Iod couples was efficient using a LED@405 nm, while Iod alone or the dyes alone could not initiate the polymerization (e.g. **Carb\_29**/Iod FC = 74%; Figure 2 (A), curve 7). Same efficiency was observed in thick samples (1.4 mm, under air) using the Carb/Iod systems, but for some dyes, the monomer conversion was low compared to the results obtained in thin samples (e.g., **Carb\_8**, Figure 2 (A), curve 2 FC = 73% vs. Figure 3 (A) curve 2 FC = 41%). This behaviour can be attributed to an internal filter effect (see also Table 2). Consequently, the studied compounds were quite efficient in photo-oxidation processes (electron transfer from Carb to Iod) to initiate a FRP in combination with Iod (the chemical mechanism is discussed below, using different techniques such as cyclic voltammetry, photoluminescence spectroscopy and photolysis experiments).

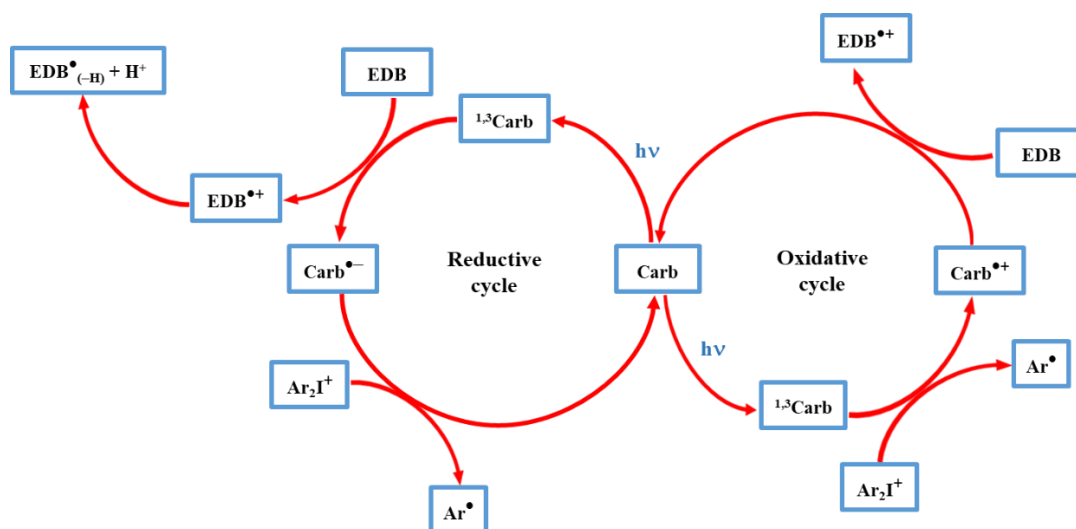
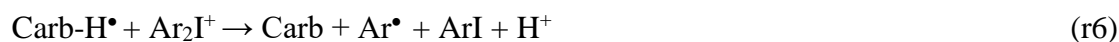
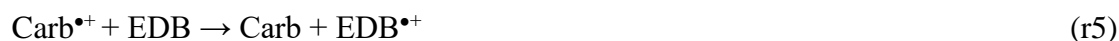
Parallel to this, 5,12-dihydroindolo[3,2-*a*]carbazole derivatives were also examined as Type-II photoinitiators with an amine (EDB), leading also to an efficient photo-reduction process for FRP. After irradiating a Carb/EDB system at 405 nm, a reaction could take place between the excited state of the dyes <sup>1</sup>Carb and EDB. Following the reactions (r3, r4), EDB•<sub>(-H)</sub> was formed and this species was responsible for the initiation of FRP. Firstly, an electron was transferred from EDB to Carb (r3), followed by a hydrogen abstraction (r4) leading to the formation of EDB•<sub>(-H)</sub> radicals responsible for initiating FRP.



Markedly, FRP of TA in the presence of the different Carb/EDB (0.1%/1% w/w) couples was efficient using LED@405 nm, while EDB alone, or Carb alone could not initiate FRP processes. Typical acrylate function conversion–time profiles are given in Figure 2 (B) for thin films (25 μm, in laminate), Figure 3 (B) for thick samples (1.4 mm, under air) and the FCs are

summarized in Table 2. High FCs could be reached in Carb/EDB systems (e.g. **Carb\_35**/EDB FC = 68%; Figure 3 (B), curve 8 using LED@405 nm).

With the regard to the three-component photoinitiating systems (PISs), in both thin (25  $\mu\text{m}$ , in laminate) (Figure 2) and thick samples (1.4 mm, under air), better performances were obtained when a third component was added to the photosensitive formulations. Indeed, using a three-component system, the maximum acrylate function conversions (FCs) and the polymerization rates ( $R_p$ ) achieved in these conditions were higher than those obtained with the two-components PISs (e.g. **Carb\_6**/Iod FC= 69% Figure 2 (A) curve 1 or **Carb\_6**/EDB FC=61% Figure 2 (B) curve 1 vs. **Carb\_6**/Iod/EDB FC= 75% Figure 2 (C) curve 1, and **Carb\_35**/Iod FC= 65% Figure 3 (A) curve 8 or **Carb\_35**/EDB FC=68% Figure 3 (B) curve 8 vs. **Carb\_35**/Iod/EDB FC=83% Figure 3 (C) curve 8). This fact was also partly ascribed to the formation of a charge transfer complex (CTC) between Iod and EDB which is able to generate reactive species when it absorbs light. Additionally,  $\text{Carb}^{\bullet+}$  can react with EDB (r5) or  $\text{Carb-H}^{\bullet}$  with Iod (r6) (see also Scheme 11). Finally, the dye can be regenerated (See also scheme 11 and see the steady state photolysis results below).[3,83,101–103]



**Scheme 11.** Proposed photoredox catalytic cycle for the three-component Carb/Iod/EDB system.

Overall, in this series of dyes, seven of them could furnish monomer conversions higher than 87%, namely **Carb\_1**, **Carb\_24**, **Carb\_25**, **Carb\_27**, **Carb\_29**, **Carb\_30** and **Carb\_36** (See Table 2). Concerning **Carb\_1**, **Carb\_24**, **Carb\_30** and **Carb\_36**, the high reactivity of

these four dyes can be assigned to the high molar extinction coefficients of these dyes at 405 nm. On the opposite, **Carb\_25**, **Carb\_27** and **Carb\_29** exhibit low molar extinction coefficients at 405 nm. Their remarkable reactivities can be assigned in this case to the highly negative free energy changes determined for the electron transfer reactions. Indeed, these dyes exhibit the most negative free energy changes for the electron transfer reaction of the series. Therefore, high performance of the seven dyes is the result of high molar extinction coefficients at 405 nm or appropriate redox properties providing highly negative free energy changes for the electron transfer from the dye towards the iodonium salt.

**Table 2.** Final Acrylate Monomer Conversion (FC) for TA after 100 s.

	Thickness= 25 $\mu$ m (In laminate)			Thickness= 1.4 mm (Under air)		
	PI/Iod (0,1%/1% w/w)	PI/EDB (0,1%/1% w/w)	PI/Iod/EDB (0,1%/1%/1% w/w/w)	PI/Iod (0,1%/1% w/w)	PI/EDB (0,1%/1% w/w)	PI/Iod/EDB (0,1%/1%/1% w/w/w)
<b>Carb_1</b>	56%	48%	58%	77%	78%	89%
<b>Carb_2</b>	62%	54%	62%	60%	79%	78%
<b>Carb_3</b>	72%	63%	70%	53%	63%	75%
<b>Carb_4</b>	69%	59%	71%	56%	79%	51%
<b>Carb_5</b>	70%	48%	75%	68%	69%	74%
<b>Carb_6</b>	69%	61%	75%	55%	75%	54%
<b>Carb_7</b>	45%	14%	66%	20%	11%	77%
<b>Carb_8</b>	73%	53%	80%	41%	34%	45%
<b>Carb_9</b>	66%	60%	66%	34%	11%	74%
<b>Carb_10</b>	48%	53%	61%	10%	1%	16%
<b>Carb_11</b>	72%	55%	82%	11%	32%	25%
<b>Carb_12</b>	61%	72%	71%	69%	46%	39%
<b>Carb_13</b>	71%	62%	73%	49%	77%	76%
<b>Carb_14</b>	75%	63%	76%	63%	72%	35%
<b>Carb_15</b>	60%	56%	64%	61%	74%	63%
<b>Carb_17</b>	64%	31%	65%	61%	28%	34%
<b>Carb_18</b>	70%	66%	74%	38%	41%	41%
<b>Carb_24</b>	67%	31%	71%	79%	56%	91%
<b>Carb_25</b>	1%	42%	71%	15%	6%	86%
<b>Carb_26</b>	87%	49%	86%	64%	7%	80%
<b>Carb_27</b>	87%	39%	93%	70%	5%	86%
<b>Carb_28</b>	73%	63%	73%	69%	12%	64%
<b>Carb_29</b>	74%	63%	74%	63%	14%	91%
<b>Carb_30</b>	68%	41%	64%	70%	9%	87%
<b>Carb_31</b>	58%	68%	60%	78%	78%	82%

<b>Carb_32</b>	65%	66%	68%	50%	81%	77%
<b>Carb_33</b>	71%	84%	71%	35%	70%	71%
<b>Carb_34</b>	90%	89%	89%	53%	72%	75%
<b>Carb_35</b>	49%	79%	52%	65%	68%	83%
<b>Carb_36</b>	69%	62%	73%	73%	78%	87%
<b>Iod/EDB (1%/1% w/w)</b>		52%			66%	

### 3.3. Chemical mechanisms

#### 3.3.1. Steady state photolysis

Steady-state photolysis of the Carb/Iod ( $10^{-2}$  M), Carb/EDB ( $10^{-2}$  M) and Carb/Iod/EDB ( $10^{-2}$  M/  $10^{-2}$  M) systems was performed in chloroform under light irradiation, using a LED@375 nm. It is remarkable that, for example the photolysis of **Carb\_29**/Iod system was very efficient (See Figure 4 (A)) with the formation of new photoproducts (characterized by a significant new absorption for  $\lambda > 395$  nm) which is due to the Carb/Iod interaction. Isobestic points were found suggesting a clean process without side reactions. In the same way, photolysis of the **Carb\_29**/EDB system was also efficient (Figure 4 (B)) but slower than that with the iodonium salt, which can in addition suggest a photochemical reaction between the studied dyes and EDB, in agreement with the results observed in the photopolymerization experiments. Indeed, photolysis of **Carb\_29** in the presence of the Iod/EDB couple (Figure 4 (C)) was lower than that observed with Iod or EDB alone (Figure 4 (A, B), clearly showing that **Carb\_29** is regenerated in the three-component system (see also the consumption of **Carb\_29** with Iod, EDB, and Iod/EDB in Figure 4 (D)).

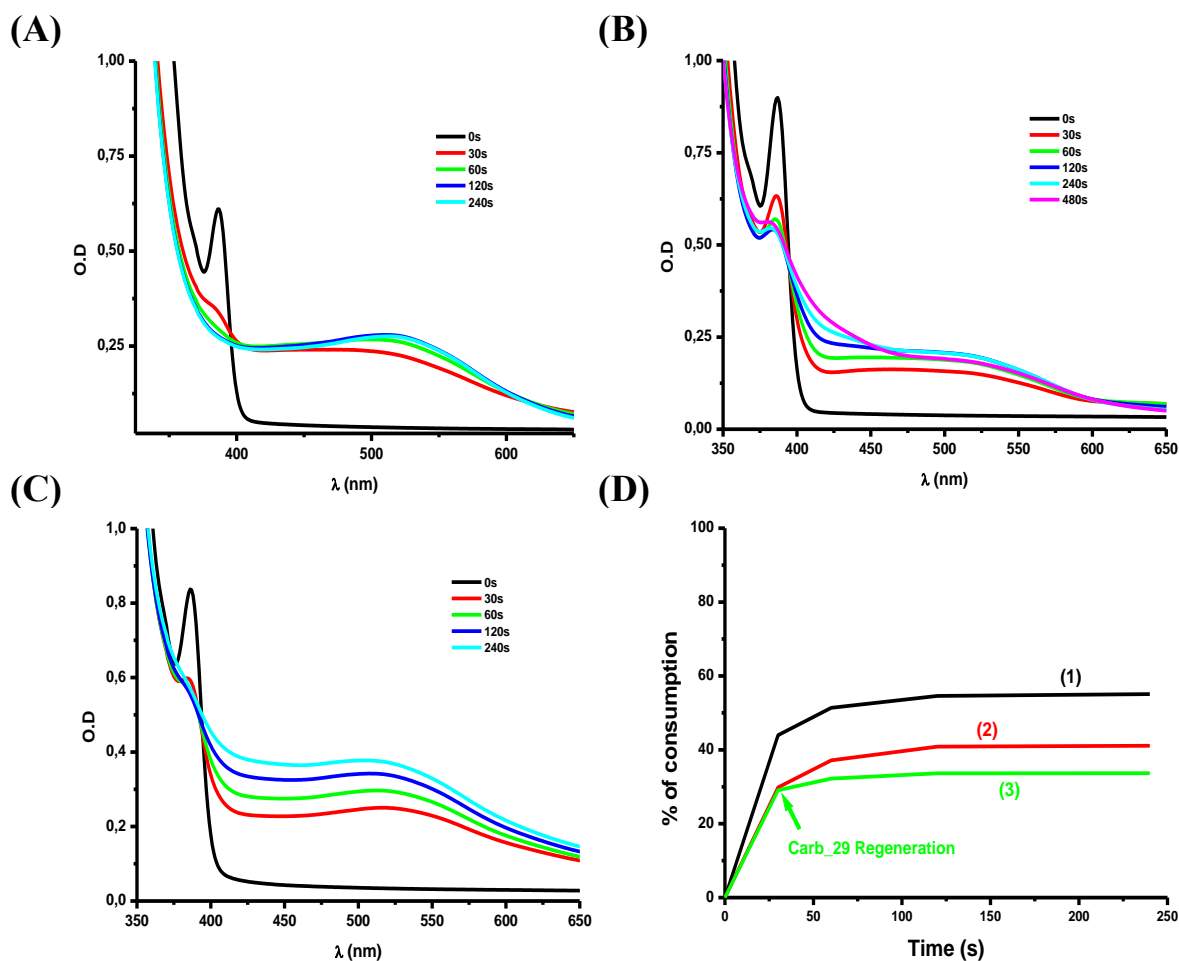


**Figure 4.** Photolysis of **Carb\_29** in chloroform upon irradiation with a LED@375 nm (A) with Iod ( $10^{-2}$  M); (B) with EDB ( $10^{-2}$  M); (C) with Iod/EDB ( $10^{-2}$  M/ $10^{-2}$  M); and (D) Consumption of **Carb\_29**: (1) with Iod salt; (2) with EDB; and (3) with Iod/EDB.

### 3.3.2. Fluorescence quenching

In order to better understand the interaction existing between the studied dyes and the iodonium salt (Iod), fluorescence quenching experiments were carried out in chloroform. For example, as shown in Figure 5, a fast fluorescence quenching process of **Carb\_30** by Iod was detected (see Figure 5 and Table 3); this clearly shows a very strong interaction of **Carb\_30** (and even the other dyes) with the iodonium salt ((r1) and (r2)). The associated electron transfer quantum yields ( $\Phi_{\text{et}}$ ) were determined according to the following equation:  $\Phi_{\text{et}} = k_{\text{sv}}[\text{Iod}]/(1 + k_{\text{sv}}[\text{Iod}])$  and high  $\Phi_{\text{et}}$  are found (e.g.,  $\Phi = 0.69$  for **Carb\_30**, Table 3).

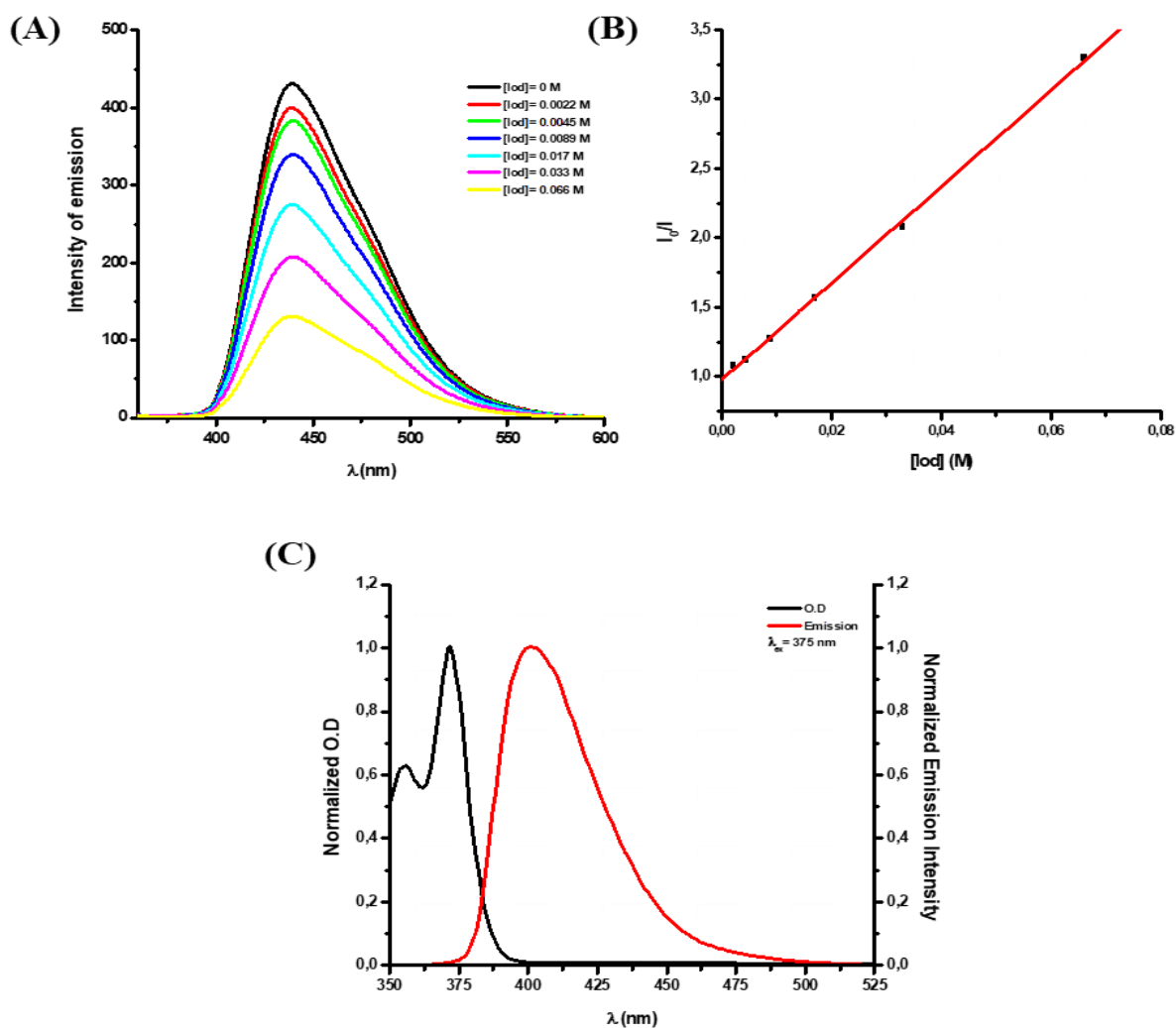


**Figure 5.** (A) Quenching of  $^1\text{Carb}_{30}$  by Iod in chloroform. (B) Determination of the Stern-Volmer coefficient. (C) UV-visible absorption and emission spectra  $\text{Carb}_{27}$  in chloroform.

In addition, interaction between Carb/Iod (or Carb/EDB) was investigated through the evaluation of the free energy changes ( $\Delta G_{\text{Iod}}$  or  $\Delta G_{\text{EDB}}$ , respectively) for the electron transfer reactions.[100,104–106] According to the equation (1) ( $\Delta G_{\text{et}} = E_{\text{ox}} - E_{\text{red}} - E^* + C$ ),  $\Delta G_{\text{Iod}}$  or  $\Delta G_{\text{EDB}}$  were determined from the oxidation potential  $E_{\text{ox}}$  (or the reduction potentials) of the studied dyes and their singlet excited state energy ( $E_{\text{S1}}$ ) could be calculated from the crossing point of the UV-visible absorption and the fluorescence spectra, as shown in Figure 5 (C). The different results are gathered in Table 3). Favorable  $\Delta G$  were found in agreement with the strong  $^1\text{Carb}/\text{Iod}$  or  $^1\text{Carb}/\text{EDB}$  interaction observed above in photopolymerization experiments.

**Table 3.** Parameters characterizing the chemical mechanisms associated with the studied dyes in chloroform.

PI	$E_{S1}$ (eV)	$E_{ox}$ (V)	$E_{red}$ (V)	$\Delta G_{S1(PI/Iod)}$ (eV) <sup>a</sup>	$\Delta G_{S1(PI/EDB)}$ (eV) <sup>b</sup>	$K_{sv(Iod)}$ (M <sup>-1</sup> ) <sup>c</sup>	$\Phi^{et(S1)_{Iod}}$
Carb_1	-	1.19	-	-	-	-	-
Carb_2	-	1.24	-	-	-	-	-
Carb_3	-	0.99	-1.02	-	-	-	-
Carb_4	-	0.99	-	-	-	-	-
Carb_5	-	1.09	-1.19	-	-	-	-
Carb_6	-	1.10	-1.08	-	-	-	-
Carb_7	-	0.74	-1.02	-	-	-	-
Carb_8	2.30	1.18	-1.10	-0.42	-0.2	53.33	0.64
Carb_9	2.35	1.16	-1.17	-0.49	-0.18	38.75	0.56
Carb_10	2.05	1.18	-0.98	-0.17	-0.07	22.92	0.43
Carb_11	2.51	1.20	-1.01	-0.61	-0.5	6.43	0.17
Carb_12	2.48	1.50	-1.00	-0.28	-0.48	4.04	0.11
Carb_13	-	1.04	-0.96	-	-	-	-
Carb_14	-	1.03	-0.97	-	-	-	-
Carb_15	-	1.03	-0.99	-	-	-	-
Carb_17	2.37	1.02	-1.14	-0.65	-0.23	7.45	0.11
Carb_18	2.26	1.10	-0.98	-0.46	-0.28	7.59	0.21
Carb_24	3.03	0.92	-1.08	-1.41	-0.95	41.28	0.57
Carb_25	3.31	1.16	-1.12	-1.45	-1.19	25.59	0.62
Carb_26	3.20	0.96	-0.99	-1.54	-1.21	8.69	0.26
Carb_27	3.24	0.95	-1.10	-1.59	-1.14	21.73	0.58
Carb_28	3.25	0.93	-1.03	-1.62	-1.22	18.43	0.54
Carb_29	3.12	1.36	-1.03	-1.06	-1.09	39.52	0.71
Carb_30	3.06	1.34	-1.04	-1.02	-1.02	34.75	0.69
Carb_31	-	1.01	-1.05	-	-	-	-
Carb_32	2.57	1.18	-1.07	-0.69	-0.5	12.02	0.29
Carb_33	-	1.06	-1.07	-	-	-	-
Carb_34	2.56	1.14	-1.06	-0.72	-0.5	15.15	0.34
Carb_35	2.51	1.17	-1.12	-0.64	-0.39	4.59	0.13
Carb_36	-	1.06	-1.13	-	-	-	-

a: evaluated from  $\Delta G_{S1(PI/Iod)} = E_{ox} - E_{red}(Iod) - E_{S1}$ ;  $E_{red}(Iod) = -0.7$  V.

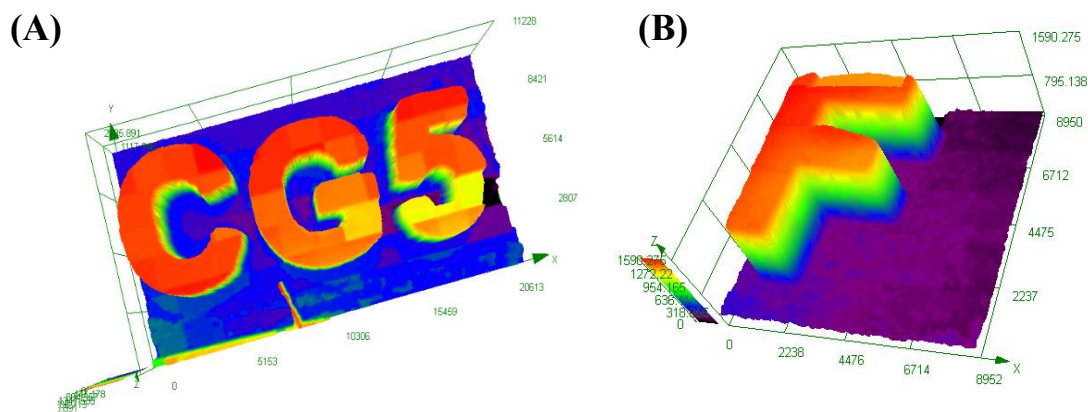
b: evaluated from  $\Delta G_{S1(PI/EDB)} = E_{ox}(EDB) - E_{red} - E_{S1}$ ;  $E_{ox}(EDB) = 1$  V.

c: Stern-Volmer coefficient ( $K_{sv}$ ); slope of the quenching curve:  $I/I_0 = (1 + k_{sv}[Iod])$ .



### 3.4. 3D printing experiments













Due to their high photoreactivity during the FRP of TA, the two three-component systems **Carb\_5/Iod/EDB** and **Carb\_24/Iod/EDB** were selected for 3D printing experiments upon laser diode irradiation at 405 nm. This experiment was carried out under air. As shown in the Figure 6, 3D patterns exhibiting a significant thickness could be obtained, together with a high spatial resolution (polymerization process is only produced in the irradiated area). Noticeably, very short irradiation times ( $\sim 2$  min.) were necessary to generate the different 3D patterns. ( $\sim 2$  min.). The different letters (C, G, 5 and F) were characterized by numerical optical microscopy (See Figure 6).



**Figure 6.** 3D patterns obtained upon exposure to a laser diode @405 nm: characterization by numerical microscopy; (A): **Carb\_5/Iod/EDB** (0.1%/1%/1% w/w/w) in Ebecryl40 (thickness = 2200  $\mu\text{m}$ ); (B): **Carb\_24/Iod/EDB** (0.1%/1%/1% w/w/w) in Ebecryl40 (thickness = 1590 $\mu\text{m}$ ).

### 3.5. Near-UV conveyor experiments for access to photocomposites

Photocomposite materials were synthesized by impregnation of glass fibers by TA (50% glass fibers/ 50% resin; thickness of  $\sim 3$  mm) and then irradiation of the sample. The results show that the studied dyes were able to fully cure the composites. An efficient curing polymerization was observed i.e. the surface became tack-free after only one pass of irradiation with the LED @395 nm (See Figure 7) This character is observed at the bottom of the sample but only after some passes.

			Number of passes to obtained tack-free			
			Surface	Bottom	Thickness (mm)	
(1)		→		1	20	3.15
(2)		→		3	23	3.63
(3)		→		3	21	3.09
(4)		→		1	15	3.15
(5)		→		1	15	3.22
(6)		→		1	14	2.99

**Figure 7.** Photocomposites produced by FRP experiments of acrylate monomer (TA) using a LED conveyor @395 nm Carb/Iod/EDB (0.1%/1%/1% w/w/w): (1) **Carb\_5**, (2) **Carb\_11**, (3) **Carb\_13**, (4) **Carb\_24**, (5) **Carb\_29** and (6) **Carb\_36**.

## Conclusion

In this study, a series of 36 new dyes never reported in the literature was synthesized for the elaboration of new high-performance photoinitiating systems capable to efficiently initiate free radical photopolymerizations (FRP) of acrylates upon blue LED irradiation. The FRP results were explained and discussed by a general mechanism proposed using different characterization techniques such as steady-state photolysis, fluorescence quenching, and cyclic voltammetry. It was also noted that, both good light absorption properties and excellent photochemical reactivity in the excited state processes are required for the dyes to reach efficient photoinitiating systems. In addition, the good performance of the investigated dyes paved the way for their use in 3D printing technology, which allows the generation of 3D thick

patterns using a laser diode at 405 nm, and the synthesis of thick glass fiber photocomposites. Development of new high-performance photoinitiating systems is currently under progress.

## Acknowledgments

Aix Marseille University and the Centre National de la Recherche Scientifique (CNRS) are acknowledged for financial supports.

## Conflicts of Interest

The authors declare no conflict of interest.

## References

- [1] A. Bagheri, J. Jin, Photopolymerization in 3D Printing, *ACS Appl. Polym. Mater.* 1 (2019) 593–611. <https://doi.org/10.1021/acsapm.8b00165>.
- [2] A. Andreu, P.-C. Su, J.-H. Kim, C.S. Ng, S. Kim, I. Kim, J. Lee, J. Noh, A.S. Subramanian, Y.-J. Yoon, 4D printing materials for vat photopolymerization, *Additive Manufacturing.* 44 (2021) 102024. <https://doi.org/10.1016/j.addma.2021.102024>.
- [3] H. Chen, G. Noirbent, Y. Zhang, K. Sun, S. Liu, D. Brunel, D. Gigmes, B. Graff, F. Morlet-Savary, P. Xiao, F. Dumur, J. Lalevée, Photopolymerization and 3D/4D applications using newly developed dyes: Search around the natural chalcone scaffold in photoinitiating systems, *Dyes and Pigments.* 188 (2021) 109213. <https://doi.org/10.1016/j.dyepig.2021.109213>.
- [4] N. Corrigan, J. Yeow, P. Judzewitsch, J. Xu, C. Boyer, Seeing the Light: Advancing Materials Chemistry through Photopolymerization, *Angewandte Chemie International Edition.* 58 (2019) 5170–5189. <https://doi.org/10.1002/anie.201805473>.
- [5] J.P. Fouassier, X. Allonas, D. Burget, Photopolymerization reactions under visible lights: principle, mechanisms and examples of applications, *Progress in Organic Coatings.* 47 (2003) 16–36. [https://doi.org/10.1016/S0300-9440\(03\)00011-0](https://doi.org/10.1016/S0300-9440(03)00011-0).
- [6] N. Zivic, P.K. Kuroishi, F. Dumur, D. Gigmes, A.P. Dove, H. Sardon, Recent Advances and Challenges in the Design of Organic Photoacid and Photobase Generators for Polymerizations, *Angewandte Chemie International Edition.* 58 (2019) 10410–10422. <https://doi.org/10.1002/anie.201810118>.
- [7] A. Santini, I.T. Gallegos, C.M. Felix, Photoinitiators in Dentistry: A Review, *Prim Dent J.* 2 (2013) 30–33. <https://doi.org/10.1308/205016814809859563>.
- [8] H. Arikawa, H. Takahashi, T. Kanie, S. Ban, Effect of various visible light photoinitiators on the polymerization and color of light-activated resins, *Dental Materials Journal.* 28 (2009) 454–460. <https://doi.org/10.4012/dmj.28.454>.
- [9] S.H. Dickens, J.W. Stansbury, K.M. Choi, C.J.E. Floyd, Photopolymerization Kinetics of Methacrylate Dental Resins, *Macromolecules.* 36 (2003) 6043–6053. <https://doi.org/10.1021/ma021675k>.
- [10] T. Dikova, J. Maximov, V. Todorov, G. Georgiev, V. Panov, Optimization of Photopolymerization Process of Dental Composites, *Processes.* 9 (2021) 779. <https://doi.org/10.3390/pr9050779>.

- [11] A. Maffezzoli, A.D. Pietra, S. Rengo, L. Nicolais, G. Valletta, Photopolymerization of dental composite matrices, *Biomaterials*. 15 (1994) 1221–1228. [https://doi.org/10.1016/0142-9612\(94\)90273-9](https://doi.org/10.1016/0142-9612(94)90273-9).
- [12] M.G. Neumann, C.C. Schmitt, G.C. Ferreira, I.C. Corrêa, The initiating radical yields and the efficiency of polymerization for various dental photoinitiators excited by different light curing units, *Dental Materials*. 22 (2006) 576–584. <https://doi.org/10.1016/j.dental.2005.06.006>.
- [13] M. Topa, J. Ortyl, Moving Towards a Finer Way of Light-Cured Resin-Based Restorative Dental Materials: Recent Advances in Photoinitiating Systems Based on Iodonium Salts, *Materials*. 13 (2020) 4093. <https://doi.org/10.3390/ma13184093>.
- [14] F. Yoshino, A. Yoshida, Effects of blue-light irradiation during dental treatment, *Jpn Dent Sci Rev*. 54 (2018) 160–168. <https://doi.org/10.1016/j.jdsr.2018.06.002>.
- [15] I. Dika, F. Diot, V. Bardinal, J.-P. Malval, C. Ecoffet, A. Bruyant, D. Barat, B. Reig, J.-B. Doucet, T. Camps, O. Soppera, Near infrared photopolymer for micro-optics applications, *Journal of Polymer Science*. 58 (2020) 1796–1809. <https://doi.org/10.1002/pol.20200106>.
- [16] C. Dietlin, S. Schweizer, P. Xiao, J. Zhang, F. Morlet-Savary, B. Graff, J.-P. Fouassier, J. Lalevée, Photopolymerization upon LEDs: new photoinitiating systems and strategies, *Polym. Chem*. 6 (2015) 3895–3912. <https://doi.org/10.1039/C5PY00258C>.
- [17] P. Xiao, J. Zhang, F. Dumur, M.A. Tehfe, F. Morlet-Savary, B. Graff, D. Gignes, J.P. Fouassier, J. Lalevée, Visible light sensitive photoinitiating systems: Recent progress in cationic and radical photopolymerization reactions under soft conditions, *Progress in Polymer Science*. 41 (2015) 32–66. <https://doi.org/10.1016/j.progpolymsci.2014.09.001>.
- [18] M.-A. Tehfe, F. Dumur, P. Xiao, M. Delgove, B. Graff, J.-P. Fouassier, D. Gignes, J. Lalevée, Chalcone derivatives as highly versatile photoinitiators for radical, cationic, thiol–ene and IPN polymerization reactions upon exposure to visible light, *Polym. Chem*. 5 (2014) 382–390. <https://doi.org/10.1039/C3PY00922J>.
- [19] H. Mokbel, J. Toufaily, T. Hamieh, F. Dumur, D. Campolo, D. Gignes, J.P. Fouassier, J. Ortyl, J. Lalevée, Specific cationic photoinitiators for near UV and visible LEDs: Iodonium versus ferrocenium structures, *Journal of Applied Polymer Science*. 132 (2015). <https://doi.org/10.1002/app.42759>.
- [20] J. Lalevée, S. Telitel, P. Xiao, M. Lepeltier, F. Dumur, F. Morlet-Savary, D. Gignes, J.-P. Fouassier, Metal and metal-free photocatalysts: mechanistic approach and application as photoinitiators of photopolymerization, *Beilstein J. Org. Chem*. 10 (2014) 863–876. <https://doi.org/10.3762/bjoc.10.83>.
- [21] S. Liu, D. Brunel, K. Sun, Y. Xu, F. Morlet-Savary, B. Graff, P. Xiao, F. Dumur, J. Lalevée, A monocomponent bifunctional benzophenone–carbazole type II photoinitiator for LED photoinitiating systems, *Polym. Chem*. 11 (2020) 3551–3556. <https://doi.org/10.1039/D0PY00644K>.
- [22] T.-L. Huang, Y.-H. Li, Y.-C. Chen, Benzophenone derivatives as novel organosoluble visible light Type II photoinitiators for UV and LED photoinitiating systems, *Journal of Polymer Science*. 58 (2020) 2914–2925. <https://doi.org/10.1002/pol.20200437>.
- [23] X. Qin, G. Ding, Y. Gong, C. Jing, G. Peng, S. Liu, L. Niu, S. Zhang, Z. Luo, H. Li, F. Gao, Stilbene-benzophenone dyads for free radical initiating polymerization of methyl methacrylate under visible light irradiation, *Dyes and Pigments*. 132 (2016) 27–40. <https://doi.org/10.1016/j.dyepig.2016.04.035>.
- [24] S. Liu, D. Brunel, G. Noirbent, A. Mau, H. Chen, F. Morlet-Savary, B. Graff, D. Gignes, P. Xiao, F. Dumur, J. Lalevée, New multifunctional benzophenone-based photoinitiators with high migration stability and their applications in 3D printing, *Mater. Chem. Front*. 5 (2021) 1982–1994. <https://doi.org/10.1039/D0QM00885K>.

- [25] J. Lalevée, M.-A. Tehfe, F. Dumur, D. Gimes, B. Graff, F. Morlet-Savary, J.-P. Fouassier, Light-Harvesting Organic Photoinitiators of Polymerization, *Macromolecular Rapid Communications*. 34 (2013) 239–245. <https://doi.org/10.1002/marc.201200578>.
- [26] M.-A. Tehfe, F. Dumur, B. Graff, F. Morlet-Savary, D. Gimes, J.-P. Fouassier, J. Lalevée, Design of new Type I and Type II photoinitiators possessing highly coupled pyrene–ketone moieties, *Polym. Chem.* 4 (2013) 2313–2324. <https://doi.org/10.1039/C3PY21079K>.
- [27] M.-A. Tehfe, F. Dumur, B. Graff, J.-L. Clément, D. Gimes, F. Morlet-Savary, J.-P. Fouassier, J. Lalevée, New Cleavable Photoinitiator Architecture with Huge Molar Extinction Coefficients for Polymerization in the 340–450 nm Range., *Macromolecules*. 46 (2013) 736–746. <https://doi.org/10.1021/ma3024359>.
- [28] P. Xiao, F. Dumur, B. Graff, D. Gimes, J.P. Fouassier, J. Lalevée, Variations on the Benzophenone Skeleton: Novel High Performance Blue Light Sensitive Photoinitiating Systems, *Macromolecules*. 46 (2013) 7661–7667. <https://doi.org/10.1021/ma401766v>.
- [29] J. Zhang, N. Zivic, F. Dumur, P. Xiao, B. Graff, D. Gimes, J.P. Fouassier, J. Lalevée, A benzophenone-naphthalimide derivative as versatile photoinitiator of polymerization under near UV and visible lights, *Journal of Polymer Science Part A: Polymer Chemistry*. 53 (2015) 445–451. <https://doi.org/10.1002/pola.27451>.
- [30] E. Andrezajewska, K. Grajek, Recent advances in photo-induced free-radical polymerization, *MOJ Polym Sci.* 1 (2017) 58–60. <https://doi.org/10.15406/mojps.2017.01.00009>.
- [31] F. Dumur, Recent advances on pyrene-based photoinitiators of polymerization, *European Polymer Journal*. 126 (2020) 109564. <https://doi.org/10.1016/j.eurpolymj.2020.109564>.
- [32] F. Dumur, Recent advances on ferrocene-based photoinitiating systems, *European Polymer Journal*. 147 (2021) 110328. <https://doi.org/10.1016/j.eurpolymj.2021.110328>.
- [33] F. Dumur, Recent advances on visible light photoinitiators of polymerization based on Indane-1,3-dione and related derivatives, *European Polymer Journal*. 143 (2021) 110178. <https://doi.org/10.1016/j.eurpolymj.2020.110178>.
- [34] F. Dumur, Recent advances on iron-based photoinitiators of polymerization, *European Polymer Journal*. 139 (2020) 110026. <https://doi.org/10.1016/j.eurpolymj.2020.110026>.
- [35] F. Dumur, Recent Advances on Visible Light Metal-Based Photocatalysts for Polymerization under Low Light Intensity, *Catalysts*. 9 (2019). <https://doi.org/10.3390/catal9090736>.
- [36] F. Dumur, Recent advances on perylene-based photoinitiators of polymerization, *European Polymer Journal*. 159 (2021) 110734. <https://doi.org/10.1016/j.eurpolymj.2021.110734>.
- [37] N. Giacoletto, M. Ibrahim-Ouali, F. Dumur, Recent advances on squaraine-based photoinitiators of polymerization, *European Polymer Journal*. 150 (2021) 110427. <https://doi.org/10.1016/j.eurpolymj.2021.110427>.
- [38] N. Giacoletto, F. Dumur, Recent Advances in bis-Chalcone-Based Photoinitiators of Polymerization: From Mechanistic Investigations to Applications, *Molecules*. 26 (2021) 3192. <https://doi.org/10.3390/molecules26113192>.
- [39] M. Ibrahim-Ouali, F. Dumur, Recent Advances on Chalcone-based Photoinitiators of Polymerization, *European Polymer Journal*. (2021) 110688. <https://doi.org/10.1016/j.eurpolymj.2021.110688>.
- [40] G. Noirbent, F. Dumur, Recent advances on naphthalic anhydrides and 1,8-naphthalimide-based photoinitiators of polymerization, *European Polymer Journal*. 132 (2020) 109702. <https://doi.org/10.1016/j.eurpolymj.2020.109702>.

- [41] G. Noirbent, F. Dumur, Recent Advances on Copper Complexes as Visible Light Photoinitiators and (Photo) Redox Initiators of Polymerization, *Catalysts*. 10 (2020). <https://doi.org/10.3390/catal10090953>.
- [42] C. Pigot, G. Noirbent, D. Brunel, F. Dumur, Recent advances on push–pull organic dyes as visible light photoinitiators of polymerization, *European Polymer Journal*. 133 (2020) 109797. <https://doi.org/10.1016/j.eurpolymj.2020.109797>.
- [43] F. Dumur, Recent Advances on Visible Light Thiophene-based Photoinitiators of Polymerization, *European Polymer Journal*. (2022) 111120. <https://doi.org/10.1016/j.eurpolymj.2022.111120>.
- [44] F. Dumur, Recent Advances on Anthracene-based Photoinitiators of Polymerization, *European Polymer Journal*. (2022) 111139. <https://doi.org/10.1016/j.eurpolymj.2022.111139>.
- [45] F. Dumur, Recent advances on visible light Triphenylamine-based photoinitiators of polymerization, *European Polymer Journal*. 166 (2022) 111036. <https://doi.org/10.1016/j.eurpolymj.2022.111036>.
- [46] F. Dumur, Recent advances on visible light Phenothiazine-based photoinitiators of polymerization, *European Polymer Journal*. 165 (2022) 110999. <https://doi.org/10.1016/j.eurpolymj.2022.110999>.
- [47] F. Dumur, Recent advances on coumarin-based photoinitiators of polymerization, *European Polymer Journal*. 163 (2022) 110962. <https://doi.org/10.1016/j.eurpolymj.2021.110962>.
- [48] P. Xiao, F. Dumur, T.T. Bui, F. Goubard, B. Graff, F. Morlet-Savary, J.P. Fouassier, D. Gigmes, J. Lalevée, Panchromatic Photopolymerizable Cationic Films Using Indoline and Squaraine Dye Based Photoinitiating Systems, *ACS Macro Lett.* 2 (2013) 736–740. <https://doi.org/10.1021/mz400316y>.
- [49] F. Dumur, D. Gigmes, J.-P. Fouassier, J. Lalevée, Organic Electronics: An El Dorado in the Quest of New Photocatalysts for Polymerization Reactions, *Acc. Chem. Res.* 49 (2016) 1980–1989. <https://doi.org/10.1021/acs.accounts.6b00227>.
- [50] K.H. Choi, J.M. Kim, W.J. Chung, J.Y. Lee, Effects of Substitution Position of Carbazole-Dibenzofuran Based High Triplet Energy Hosts to Device Stability of Blue Phosphorescent Organic Light-Emitting Diodes, *Molecules*. 26 (2021) 2804. <https://doi.org/10.3390/molecules26092804>.
- [51] A. van Dijken, J.J.A.M. Bastiaansen, N.M.M. Kiggen, B.M.W. Langeveld, C. Rothe, A. Monkman, I. Bach, P. Stössel, K. Brunner, Carbazole Compounds as Host Materials for Triplet Emitters in Organic Light-Emitting Diodes: Polymer Hosts for High-Efficiency Light-Emitting Diodes, *J. Am. Chem. Soc.* 126 (2004) 7718–7727. <https://doi.org/10.1021/ja049771j>.
- [52] N. Blouin, A. Michaud, D. Gendron, S. Wakim, E. Blair, R. Neagu-Plesu, M. Belletête, G. Durocher, Y. Tao, M. Leclerc, Toward a Rational Design of Poly(2,7-Carbazole) Derivatives for Solar Cells, *J. Am. Chem. Soc.* 130 (2008) 732–742. <https://doi.org/10.1021/ja0771989>.
- [53] F. Dumur, Carbazole-based polymers as hosts for solution-processed organic light-emitting diodes: Simplicity, efficacy, *Organic Electronics*. 25 (2015) 345–361. <https://doi.org/10.1016/j.orgel.2015.07.007>.
- [54] A. Arai, H. Sasabe, K. Nakao, Y. Masuda, J. Kido,  $\pi$ -Extended Carbazole Derivatives as Host Materials for Highly Efficient and Long-Life Green Phosphorescent Organic Light-Emitting Diodes, *Chemistry – A European Journal*. 27 (2021) 4971–4976. <https://doi.org/10.1002/chem.202005144>.

- [55] F. Dumur, L. Beouch, S. Peralta, G. Wantz, F. Goubard, D. Gigmes, Solution-processed blue phosphorescent OLEDs with carbazole-based polymeric host materials, *Organic Electronics*. 25 (2015) 21–30. <https://doi.org/10.1016/j.orgel.2015.06.013>.
- [56] D. Sun, Q. Fu, Z. Ren, W. Li, H. Li, D. Ma, S. Yan, Carbazole-based polysiloxane hosts for highly efficient solution-processed blue electrophosphorescent devices, *J. Mater. Chem. C*. 1 (2013) 5344–5350. <https://doi.org/10.1039/C3TC31108B>.
- [57] T.-T. Bui, S.K. Shah, M. Abbas, X. Sallenave, G. Sini, L. Hirsch, F. Goubard, Carbazole-Based Molecular Glasses as Hole-Transporting Materials in Solid State Dye-Sensitized Solar Cells, *ChemNanoMat*. 1 (2015) 203–210. <https://doi.org/10.1002/cnma.201500014>.
- [58] G. Puckyte, B. Schmaltz, A. Tomkeviciene, M. Degbia, J.V. Grazulevicius, H. Melhem, J. Bouclé, F. Tran-Van, Carbazole-based molecular glasses for efficient solid-state dye-sensitized solar cells, *Journal of Power Sources*. 233 (2013) 86–92. <https://doi.org/10.1016/j.jpowsour.2013.01.137>.
- [59] T.-T. Bui, F. Goubard, J. Troughton, T. Watson, Simple 3,6-bis(diphenylaminyl)carbazole molecular glasses as hole transporting materials for hybrid perovskite solar cells, *Journal of Materials Science: Materials in Electronics*. 28 (2017) 17551–17556. <https://doi.org/10.1007/s10854-017-7691-y>.
- [60] N. Berton, R. Nakar, B. Schmaltz, DMPA-containing carbazole-based hole transporting materials for perovskite solar cells: Recent advances and perspectives, *Synthetic Metals*. 252 (2019) 91–106. <https://doi.org/10.1016/j.synthmet.2019.04.004>.
- [61] M. Lepeltier, F. Appaix, Y.Y. Liao, F. Dumur, J. Marrot, T. Le Bahers, C. Andraud, C. Monnereau, Carbazole-Substituted Iridium Complex as a Solid State Emitter for Two-Photon Intravital Imaging, *Inorg. Chem*. 55 (2016) 9586–9595. <https://doi.org/10.1021/acs.inorgchem.6b01253>.
- [62] M. Khalid, A. Ali, R. Jawaria, M.A. Asghar, S. Asim, M.U. Khan, R. Hussain, M.F. ur Rehman, C.J. Ennis, M.S. Akram, First principles study of electronic and nonlinear optical properties of A–D– $\pi$ –A and D–A–D– $\pi$ –A configured compounds containing novel quinoline–carbazole derivatives, *RSC Adv*. 10 (2020) 22273–22283. <https://doi.org/10.1039/D0RA02857F>.
- [63] Mayuri M.L. Kadam, D. Patil, N. Sekar, Fluorescent carbazole based pyridone dyes – Synthesis, solvatochromism, linear and nonlinear optical properties, *Optical Materials*. 85 (2018) 308–318. <https://doi.org/10.1016/j.optmat.2018.08.072>.
- [64] W.-J. Kuo, G.-H. Hsiue, R.-J. Jeng, All Organic NLO Sol-Gel Material Containing a One-Dimensional Carbazole Chromophore, *Macromolecular Chemistry and Physics*. 202 (2001) 1782–1790. [https://doi.org/10.1002/1521-3935\(20010601\)202:9<1782::AID-MACP1782>3.0.CO;2-O](https://doi.org/10.1002/1521-3935(20010601)202:9<1782::AID-MACP1782>3.0.CO;2-O).
- [65] M. Rajeshirke, M.C. Sreenath, S. Chitrambalam, I.H. Joe, N. Sekar, Enhancement of NLO Properties in OBO Fluorophores Derived from Carbazole–Coumarin Chalcones Containing Carboxylic Acid at the N-Alkyl Terminal End, *J. Phys. Chem. C*. 122 (2018) 14313–14325. <https://doi.org/10.1021/acs.jpcc.8b02937>.
- [66] B. Souharce, C.J. Kudla, M. Forster, J. Steiger, R. Anselmann, H. Thiem, U. Scherf, Amorphous Carbazole-based (Co)polymers for OFET Application, *Macromolecular Rapid Communications*. 30 (2009) 1258–1262. <https://doi.org/10.1002/marc.200900214>.
- [67] P. Jha, S.P. Koiry, V. Saxena, P. Veerender, A. Gusain, A.K. Chauhan, A.K. Debnath, D.K. Aswal, S.K. Gupta, Air-stability and bending properties of flexible organic field-effect transistors based on poly[N-9'-heptadecanyl-2,7-carbazole-alt-5,5-(4',7'-di-2-thienyl-2',1',3'-benzothiadiazole)], *Organic Electronics*. 14 (2013) 2635–2644. <https://doi.org/10.1016/j.orgel.2013.06.031>.

- [68] C.-H. Chen, Y. Wang, T. Michinobu, S.-W. Chang, Y.-C. Chiu, C.-Y. Ke, G.-S. Liou, Donor–Acceptor Effect of Carbazole-Based Conjugated Polymer Electrets on Photoresponsive Flash Organic Field-Effect Transistor Memories, *ACS Appl. Mater. Interfaces*. 12 (2020) 6144–6150. <https://doi.org/10.1021/acsami.9b20960>.
- [69] M. Bashir, A. Bano, A.S. Ijaz, B.A. Chaudhary, Recent Developments and Biological Activities of N-Substituted Carbazole Derivatives: A Review, *Molecules*. 20 (2015) 13496–13517. <https://doi.org/10.3390/molecules200813496>.
- [70] F. Dumur, Recent advances on carbazole-based photoinitiators of polymerization, *European Polymer Journal*. 125 (2020) 109503. <https://doi.org/10.1016/j.eurpolymj.2020.109503>.
- [71] J. Zhang, D. Campolo, F. Dumur, P. Xiao, D. Gigmes, J.P. Fouassier, J. Lalevée, The carbazole-bound ferrocenium salt as a specific cationic photoinitiator upon near-UV and visible LEDs (365–405 nm), *Polym. Bull.* 73 (2016) 493–507. <https://doi.org/10.1007/s00289-015-1506-1>.
- [72] A. Al Mousawi, D.M. Lara, G. Noirbent, F. Dumur, J. Toufaily, T. Hamieh, T.-T. Bui, F. Goubard, B. Graff, D. Gigmes, J.P. Fouassier, J. Lalevée, Carbazole Derivatives with Thermally Activated Delayed Fluorescence Property as Photoinitiators/Photoredox Catalysts for LED 3D Printing Technology, *Macromolecules*. 50 (2017) 4913–4926. <https://doi.org/10.1021/acs.macromol.7b01114>.
- [73] A. Al Mousawi, P. Garra, F. Dumur, T.-T. Bui, F. Goubard, J. Toufaily, T. Hamieh, B. Graff, D. Gigmes, J.P. Fouassier, J. Lalevée, Novel Carbazole Skeleton-Based Photoinitiators for LED Polymerization and LED Projector 3D Printing, *Molecules*. 22 (2017) 2143. <https://doi.org/10.3390/molecules22122143>.
- [74] A.A. Mousawi, A. Arar, M. Ibrahim-Ouali, S. Duval, F. Dumur, P. Garra, J. Toufaily, T. Hamieh, B. Graff, D. Gigmes, J.-P. Fouassier, J. Lalevée, Carbazole-based compounds as photoinitiators for free radical and cationic polymerization upon near visible light illumination, *Photochem. Photobiol. Sci.* 17 (2018) 578–585. <https://doi.org/10.1039/C7PP00400A>.
- [75] M. Abdallah, D. Magaldi, A. Hijazi, B. Graff, F. Dumur, J.-P. Fouassier, T.-T. Bui, F. Goubard, J. Lalevée, Development of new high-performance visible light photoinitiators based on carbazole scaffold and their applications in 3d printing and photocomposite synthesis, *Journal of Polymer Science Part A: Polymer Chemistry*. 57 (2019) 2081–2092. <https://doi.org/10.1002/pola.29471>.
- [76] A. Al Mousawi, F. Dumur, P. Garra, J. Toufaily, T. Hamieh, B. Graff, D. Gigmes, J.P. Fouassier, J. Lalevée, Carbazole Scaffold Based Photoinitiator/Photoredox Catalysts: Toward New High Performance Photoinitiating Systems and Application in LED Projector 3D Printing Resins, *Macromolecules*. 50 (2017) 2747–2758. <https://doi.org/10.1021/acs.macromol.7b00210>.
- [77] S. Telitel, F. Dumur, T. Faury, B. Graff, M.-A. Tehfe, D. Gigmes, J.-P. Fouassier, J. Lalevée, New core-pyrene  $\pi$  structure organophotocatalysts usable as highly efficient photoinitiators, *Beilstein J. Org. Chem.* 9 (2013) 877–890. <https://doi.org/10.3762/bjoc.9.101>.
- [78] A.A. Mousawi, F. Dumur, P. Garra, J. Toufaily, T. Hamieh, F. Goubard, T.-T. Bui, B. Graff, D. Gigmes, J.P. Fouassier, J. Lalevée, Azahelicenes as visible light photoinitiators for cationic and radical polymerization: Preparation of photoluminescent polymers and use in high performance LED projector 3D printing resins, *Journal of Polymer Science Part A: Polymer Chemistry*. 55 (2017) 1189–1199. <https://doi.org/10.1002/pola.28476>.
- [79] S. Liu, B. Graff, P. Xiao, F. Dumur, J. Lalevée, Nitro-Carbazole Based Oxime Esters as Dual Photo/Thermal Initiators for 3D Printing and Composite Preparation,



- Macromolecular Rapid Communications. 42 (2021) 2100207.  
<https://doi.org/10.1002/marc.202100207>.
- [80] N.A. Kazin, N.S. Demina, R.A. Irgashev, E.F. Zhilina, G.L. Rusinov, Modifications of 5,12-dihydroindolo[3,2-a]carbazole scaffold via its regioselective C2,9-formylation and C2,9-acetylation, *Tetrahedron*. 75 (2019) 4686–4696.  
<https://doi.org/10.1016/j.tet.2019.07.015>.
- [81] F. Hammoud, A. Hijazi, S. Duval, J. Lalevée, F. Dumur, 5,12-Dihydroindolo[3,2-a]carbazole: A promising scaffold for the design of visible light photoinitiators of polymerization, *European Polymer Journal*. 162 (2022) 110880.  
<https://doi.org/10.1016/j.eurpolymj.2021.110880>.
- [82] F. Bureš, Fundamental aspects of property tuning in push–pull molecules, *RSC Adv*. 4 (2014) 58826–58851. <https://doi.org/10.1039/C4RA11264D>.
- [83] K. Sun, C. Pigot, Y. Zhang, T. Borjigin, F. Morlet-Savary, B. Graff, M. Nechab, P. Xiao, F. Dumur, J. Lalevée, Sunlight Induced Polymerization Photoinitiated by Novel Push–Pull Dyes: Indane-1,3-Dione, 1H-Cyclopenta[b]Naphthalene-1,3(2H)-Dione and 4-Dimethoxyphenyl-1-Allylidene Derivatives, *Macromolecular Chemistry and Physics*. n/a (2022) 2100439. <https://doi.org/10.1002/macp.202100439>.
- [84] K. Sun, S. Liu, C. Pigot, D. Brunel, B. Graff, M. Nechab, D. Gigmes, F. Morlet-Savary, Y. Zhang, P. Xiao, F. Dumur, J. Lalevée, Novel Push–Pull Dyes Derived from 1H-cyclopenta[b]naphthalene-1,3(2H)-dione as Versatile Photoinitiators for Photopolymerization and Their Related Applications: 3D Printing and Fabrication of Photocomposites, *Catalysts*. 10 (2020) 1196. <https://doi.org/10.3390/catal10101196>.
- [85] K. Sun, C. Pigot, H. Chen, M. Nechab, D. Gigmes, F. Morlet-Savary, B. Graff, S. Liu, P. Xiao, F. Dumur, J. Lalevée, Free Radical Photopolymerization and 3D Printing Using Newly Developed Dyes: Indane-1,3-Dione and 1H-Cyclopentanaphthalene-1,3-Dione Derivatives as Photoinitiators in Three-Component Systems, *Catalysts*. 10 (2020) 463. <https://doi.org/10.3390/catal10040463>.
- [86] K. Sun, S. Liu, H. Chen, F. Morlet-Savary, B. Graff, C. Pigot, M. Nechab, P. Xiao, F. Dumur, J. Lalevée, N-ethyl carbazole-1-allylidene-based push-pull dyes as efficient light harvesting photoinitiators for sunlight induced polymerization, *European Polymer Journal*. 147 (2021) 110331. <https://doi.org/10.1016/j.eurpolymj.2021.110331>.
- [87] P. Xiao, M. Frigoli, F. Dumur, B. Graff, D. Gigmes, J.P. Fouassier, J. Lalevée, Julolidine or Fluorenone Based Push–Pull Dyes for Polymerization upon Soft Polychromatic Visible Light or Green Light., *Macromolecules*. 47 (2014) 106–112. <https://doi.org/10.1021/ma402196p>.
- [88] I.R. Shaikh, Organocatalysis: Key Trends in Green Synthetic Chemistry, Challenges, Scope towards Heterogenization, and Importance from Research and Industrial Point of View, *Journal of Catalysis*. 2014 (2014) 402860. <https://doi.org/10.1155/2014/402860>.
- [89] V. da G. Oliveira, M.F. do C. Cardoso, L. da S.M. Forezi, Organocatalysis: A Brief Overview on Its Evolution and Applications, *Catalysts*. 8 (2018) 605. <https://doi.org/10.3390/catal8120605>.
- [90] S. Ardevines, E. Marqués-López, R.P. Herrera, Horizons in Asymmetric Organocatalysis: En Route to the Sustainability and New Applications, *Catalysts*. 12 (2022). <https://doi.org/10.3390/catal12010101>.
- [91] A. Carlone, L. Bernardi, Enantioselective organocatalytic approaches to active pharmaceutical ingredients – selected industrial examples, *Physical Sciences Reviews*. 4 (2019). <https://doi.org/10.1515/psr-2018-0097>.
- [92] P.I. Dalko, L. Moisan, Enantioselective Organocatalysis, *Angewandte Chemie International Edition*. 40 (2001) 3726–3748. [https://doi.org/10.1002/1521-3773\(20011015\)40:20<3726::AID-ANIE3726>3.0.CO;2-D](https://doi.org/10.1002/1521-3773(20011015)40:20<3726::AID-ANIE3726>3.0.CO;2-D).

- [93] W. Liu, H. Cao, H. Zhang, H. Zhang, K.H. Chung, C. He, H. Wang, F.Y. Kwong, A. Lei, *Organocatalysis in Cross-Coupling: DMEDA-Catalyzed Direct C–H Arylation of Unactivated Benzene*, *J. Am. Chem. Soc.* 132 (2010) 16737–16740. <https://doi.org/10.1021/ja103050x>.
- [94] J. Wilbuer, G. Schnakenburg, B. Esser, *Syntheses, Structures and Optoelectronic Properties of Spiroconjugated Cyclic Ketones*, *European Journal of Organic Chemistry*. 2016 (2016) 2404–2412. <https://doi.org/10.1002/ejoc.201600235>.
- [95] J.C. Sloop, P.D. Boyle, A.W. Fountain, C. Gomez, J.L. Jackson, W.F. Pearman, R.D. Schmidt, J. Weyand, *Novel Fluorinated Indanone, Tetralone and Naphthone Derivatives: Synthesis and Unique Structural Features*, *Applied Sciences*. 2 (2012). <https://doi.org/10.3390/app2010061>.
- [96] V. Nair, V. Nandialath, K.G. Abhilash, E. Suresh, *An efficient synthesis of indolo[3,2-a]carbazoles via the novel acid catalyzed reaction of indoles and diaryl-1,2-diones*, *Org. Biomol. Chem.* 6 (2008) 1738–1742. <https://doi.org/10.1039/B803009J>.
- [97] H. Kilic, O. Aydin, S. Bayindir, N. Saracoglu, *Condensation of Indoline with Some 1,2- and 1,3-Diketones*, *Journal of Heterocyclic Chemistry*. 53 (2016) 2096–2101. <https://doi.org/10.1002/jhet.2580>.
- [98] A. Khorshidi, N. Sadeghi, *Application of RuO<sub>2</sub> Nanoparticles as Catalyst in Preparation of Indolo[3,2-a]Carbazoles*, *J Clust Sci.* 27 (2016) 1923–1932. <https://doi.org/10.1007/s10876-016-1052-5>.
- [99] V. Bocchi, G. Palla, *Synthesis and characterization of new indole trimers and tetramers*, *Tetrahedron*. 42 (1986) 5019–5024. [https://doi.org/10.1016/S0040-4020\(01\)88053-4](https://doi.org/10.1016/S0040-4020(01)88053-4).
- [100] D. Rehm, A. Weller, *Kinetics of Fluorescence Quenching by Electron and H-Atom Transfer*, *Israel Journal of Chemistry*. 8 (1970) 259–271. <https://doi.org/10.1002/ijch.197000029>.
- [101] H. Chen, C. Regeard, H. Salmi, F. Morlet-Savary, N. Giacoletto, M. Nechab, P. Xiao, F. Dumur, J. Lalevée, *Interpenetrating polymer network hydrogels using natural based dyes initiating systems: antibacterial activity and 3D/4D performance*, *European Polymer Journal*. (2022) 111042. <https://doi.org/10.1016/j.eurpolymj.2022.111042>.
- [102] K. Sun, P. Xiao, F. Dumur, J. Lalevée, *Organic dye-based photoinitiating systems for visible-light-induced photopolymerization*, *Journal of Polymer Science*. 59 (2021) 1338–1389. <https://doi.org/10.1002/pol.20210225>.
- [103] H. Chen, G. Noirbent, S. Liu, Y. Zhang, K. Sun, F. Morlet-Savary, D. Gimes, P. Xiao, F. Dumur, J. Lalevée, *In situ generation of Ag nanoparticles during photopolymerization by using newly developed dyes-based three-component photoinitiating systems and the related 3D printing applications and their shape change behavior*, *Journal of Polymer Science*. 59 (2021) 843–859. <https://doi.org/10.1002/pol.20210154>.
- [104] S. Dadashi-Silab, S. Doran, Y. Yagci, *Photoinduced Electron Transfer Reactions for Macromolecular Syntheses*, *Chem. Rev.* 116 (2016) 10212–10275. <https://doi.org/10.1021/acs.chemrev.5b00586>.
- [105] M. Topa, F. Petko, M. Galek, M. Jankowska, R. Popielarz, J. Ortyl, *Difunctional 1H-quinolin-2-ones as spectroscopic fluorescent probes for real-time monitoring of photopolymerisation process and photosensitizers of fluorescent photopolymer resin in 3D printing*, *European Polymer Journal*. 156 (2021) 110612. <https://doi.org/10.1016/j.eurpolymj.2021.110612>.
- [106] D. Rehm, A. Weller, *Kinetik und Mechanismus der Elektronübertragung bei der Fluoreszenzlöschung in Acetonitril*, *Berichte Der Bunsengesellschaft Für Physikalische Chemie*. 73 (1969) 834–839. <https://doi.org/10.1002/bbpc.19690730818>.